




Beyond Extremality: Weak Gravity Conjecture Constraints on Gravitational Lensing in Gravity's Rainbow

Saeed Noori Gashti ^{1,*} Behnam Pourhassan ^{1,2,†} and İzzet Sakallı ^{3,‡}

¹*School of Physics, Damghan University, Damghan 3671645667, Iran*

²*Center for Theoretical Physics, Khazar University, 41 Mehseti Street, Baku, AZ1096, Azerbaijan*

³*Physics Department, Eastern Mediterranean University, Famagusta, 99628 North Cyprus, via Mersin 10, Türkiye*

(Dated: December 10, 2025)

We investigate the constraints imposed by the Weak Gravity Conjecture (WGC) on gravitational lensing in gravity's rainbow, focusing in particular on scenarios beyond extremality and on the interplay between the WGC and the Weak Cosmic Censorship Conjecture (WCCC) in the context of Reissner–Nordström–Anti-de Sitter black holes modified by rainbow gravity. Using topological methods, we first analyze the configuration of photon spheres and confirm that unstable circular photon spheres with topological charge ($\omega = -1$) exist outside the event horizon throughout the parameter space, thereby verifying the simultaneous validity of both the WGC and the WCCC. The rainbow functions $f(\varepsilon)$ and $g(\varepsilon)$, which encode Planck-scale corrections through the energy ratio ($\varepsilon = E/E_P$), modify both the spacetime metric and the extremality bound. We derive the corresponding modified extremal charge-to-mass ratio, $(q^2/m^2) > (Q^2/M^2)_{\text{ext}}$, and show that gravity's rainbow offers a natural mechanism for reconciling these two fundamental conjectures. By applying the Gauss–Bonnet theorem in conjunction with Jacobi–Maupertuis optical geometry, we compute the weak deflection angles for both photons and massive particles to second order. The rainbow function $g(\varepsilon)$ appears with powers (g^{-2}) and (g^{-4}), enhancing the deflection angle when $g(\varepsilon) < 1$, while $f(\varepsilon)$ influences only the charge-dependent contributions. At extremality, the deflection angle becomes independent of $f(\varepsilon)$, yielding a universal prediction that can be tested without specifying the form of the rainbow functions. We further find that super-extremal configurations exhibit stronger lensing effects than extremal black holes, suggesting a potential observational discriminator between WGC-satisfying naked singularities and WCCC-preserving black holes. These findings position gravitational lensing as a promising tool for probing quantum-gravity phenomenology with upcoming observational facilities.

Keywords: Weak Gravity Conjecture; Weak Cosmic Censorship Conjecture; Photon spheres; Gravitational lensing

CONTENTS

I. Introduction	2
II. R-N-AdS BH Solution in Gravity's Rainbow Framework	3
A. Action and Field Equations	4
B. Rainbow-Modified Metric Structure	4
C. Electromagnetic Field Configuration	5
D. Derivation of the Metric Function	5
E. PSs and WGC Compatibility	7
III. Gravitational Lensing Signatures and WGC Constraints at Extremality	9
A. Jacobi-Maupertuis Optical Geometry	10
B. Gaussian Curvature of the Optical Manifold	10
C. Weak Deflection Angle Derivation	11
D. WGC Implications at Extremality	13
E. Observational Predictions and Parameter Constraints	14
IV. Conclusion	16
Acknowledgments	18
References	18

* sn.gashti@du.ac.ir

† b.pourhassan@du.ac.ir

‡ izzet.sakalli@emu.edu.tr

I. INTRODUCTION

The quest for a consistent theory of quantum gravity remains one of the most profound challenges in modern theoretical physics, drawing sustained attention from researchers across high-energy physics, cosmology, and mathematical physics [1, 2]. At its core, quantum gravity seeks to reconcile the principles of quantum mechanics with those of general relativity (GR), thereby providing a unified description of spacetime at the smallest length scales where both gravitational and quantum effects become significant. While a complete formulation of quantum gravity remains elusive, substantial progress has been made through various approaches, including string theory, loop quantum gravity, asymptotic safety, and causal set theory [3–5]. Among these diverse programs, the swampland initiative has emerged as a particularly influential framework for constraining effective field theories that could arise from ultraviolet (UV) complete quantum gravity theories [6–13].

The swampland program rests on a fundamental observation: not all effective field theories that appear mathematically self-consistent at low energies can be embedded into a UV-complete theory of quantum gravity, such as string theory [6, 7]. This realization leads to a natural classification of theories into two categories. The landscape comprises theories that admit such an embedding and can thus be considered viable candidates for low-energy limits of quantum gravity. In contrast, the swampland contains theories that, despite their apparent internal consistency, fail to arise from any UV-complete gravitational theory and must therefore be excluded from physical consideration. The swampland conjectures provide a set of proposed criteria—grounded in black hole (BH) thermodynamics, holography, and string theory constructions—that aim to distinguish between these two classes [6–13].

The physical intuition underlying these conjectures draws from multiple foundational areas. BH thermodynamics, particularly the Bekenstein-Hawking entropy and information paradox, offers crucial guidance regarding the quantum nature of gravitational degrees of freedom. The holographic principle, most precisely realized through the Anti-de Sitter/Conformal Field Theory (AdS/CFT) correspondence, provides a non-perturbative definition of quantum gravity in certain spacetime backgrounds and establishes deep connections between gravitational dynamics and boundary quantum field theories [6–13]. String theory dualities and explicit compactification constructions supply concrete examples that ground the swampland criteria in calculable frameworks. Together, these threads weave a rich tapestry of constraints that any consistent theory of quantum gravity must satisfy, with implications spanning early universe cosmology, dark energy phenomenology, and particle physics beyond the Standard Model [14–83].

A cornerstone of the swampland program is the WGC, which asserts that in any consistent theory of quantum gravity coupled to a $U(1)$ gauge field, there must exist particles whose charge-to-mass ratio satisfies $q/m \geq 1$ in appropriate units. Equivalently, for charged BHs, the WGC demands the existence of states that can facilitate BH decay, preventing the formation of stable extremal remnants that would conflict with expectations from BH thermodynamics and holography [84, 85]. The conjecture effectively encodes the principle that “gravity is the weakest force”—electromagnetic repulsion must overcome gravitational attraction for sufficiently charged particles. The WGC has found applications extending well beyond its original formulation, influencing discussions of axion physics, cosmic inflation, dark matter candidates, and even the cosmological constant problem [84, 85].

Parallel to these developments in quantum gravity, the WCCC, originally proposed by Penrose, addresses a complementary question in classical gravitational physics. The WCCC posits that singularities produced by gravitational collapse are generically hidden behind event horizons, rendering them invisible to distant observers and thereby preserving the predictability of spacetime evolution. Without such protection, naked singularities would expose regions of arbitrarily high curvature to external observation, leading to breakdowns in determinism and potentially invalidating the entire framework of classical GR as a predictive theory. The WCCC has been tested extensively through gedanken experiments involving the capture of test particles by BHs, accretion of charged matter, and various perturbation analyses, with results generally supporting its validity under physically reasonable conditions [86–88].

However, a fundamental tension emerges when the WGC and WCCC are considered together in the context of charged BHs, particularly the Reissner-Nordström (RN) solution describing static, spherically symmetric BHs carrying electric charge [72, 73]. The RN metric possesses an event horizon only when the charge-to-mass ratio satisfies $Q/M \leq 1$; beyond this threshold, the horizon structure degenerates and a naked singularity appears, violating the WCCC. Conversely, the WGC requires the existence of particles with $q/m > 1$, which for standard RN BHs implies $q/m > (Q/M)_{\text{ext}}$. If such particles exist and can be absorbed by a near-extremal BH, the resulting configuration could become super-extremal ($Q > M$), exposing a naked singularity and contradicting the WCCC. This apparent conflict between two fundamental conjectures—one rooted in quantum gravity considerations and the other in classical gravitational dynamics—motivates a deeper investigation into their mutual compatibility and the conditions under which both can be simultaneously satisfied [89–91].

Recent theoretical work has identified several mechanisms that could reconcile the WGC and WCCC. The inclusion of additional matter fields, such as quintessence or dark matter components, modifies the extremality bound and can prevent overcharging [72, 73, 89–91]. Similarly, spacetimes with cosmological constants (either positive or negative) alter the horizon structure and shift the critical charge-to-mass ratio at which extremality occurs. Modified gravity theories, including those with higher-curvature corrections, introduce additional parameters that influence both the WGC bound and the conditions for cosmic censorship. These investigations suggest that the tension between the WGC and WCCC may be an artifact of

oversimplified models, and that more realistic scenarios incorporating quantum gravity effects naturally accommodate both conjectures.

Gravity's rainbow represents one such framework incorporating quantum gravity modifications into the spacetime geometry [92, 93]. Originally motivated by doubly special relativity and deformed dispersion relations arising in loop quantum gravity and string theory contexts, gravity's rainbow introduces energy-dependent rainbow functions $f(\varepsilon)$ and $g(\varepsilon)$ that modify the metric components according to the probe particle's energy relative to the Planck scale [94, 95]. These functions satisfy the infrared limit $\lim_{\varepsilon \rightarrow 0} f(\varepsilon) = \lim_{\varepsilon \rightarrow 0} g(\varepsilon) = 1$, recovering standard GR when probe energies are much smaller than the Planck energy E_P . The rainbow framework has been applied to numerous BH solutions, revealing modifications to thermodynamic properties, quasi-normal modes, Hawking radiation spectra, and geodesic structures [96, 97]. Crucially for the present work, gravity's rainbow alters the extremality condition for charged BHs, providing a natural mechanism for shifting the WGC bound while preserving cosmic censorship.

Gravitational lensing serves as one of the most powerful observational probes for testing gravitational theories and constraining BH parameters [98, 99]. The deflection of light by massive objects, first predicted by GR and confirmed during the 1919 solar eclipse, has evolved into a precision tool encompassing weak lensing surveys, strong lensing time delays, and BH shadow observations [100]. The Gauss-Bonnet (GB) theorem, combined with the Jacobi-Maupertuis optical geometry formalism pioneered by Gibbons and Werner, provides an elegant geometric framework for calculating deflection angles by integrating Gaussian curvature over appropriately defined optical manifolds [101, 102]. This approach has been extended to numerous BH spacetimes, including those with rotation, charge, and various matter surroundings, enabling analytical treatment of lensing phenomena across diverse theoretical scenarios [103, 104].

Photon spheres (PSs)—the unstable circular orbits of massless particles around compact objects—provide additional geometric information about BH spacetimes and connect naturally to both shadow observations and gravitational lensing. The topological classification of PSs, assigning winding numbers or topological charges that encode stability properties, has emerged as a fruitful approach for characterizing BH geometries. The existence of an unstable PS outside the event horizon serves as a necessary condition for BH nature, as naked singularities typically lack such structures or exhibit qualitatively different PS configurations. This connection makes PS analysis a valuable complement to direct horizon studies when assessing whether a given spacetime represents a BH or a naked singularity [89–91, 105–109].

The primary motivation for the present work stems from the desire to establish observational signatures that can discriminate between WGC-compatible and WCCC-compatible configurations in gravity's rainbow. While both conjectures address fundamental questions about quantum gravity and spacetime structure, they have remained largely theoretical constructs with limited connection to observable phenomena. Gravitational lensing, with its sensitivity to spacetime geometry and upcoming observational capabilities through facilities such as the Square Kilometre Array (SKA) and next-generation Event Horizon Telescope (ngEHT), offers a promising pathway toward empirical tests. By deriving explicit deflection angle formulas for Reissner–Nordström–AdS (R-N-AdS) BHs modified by gravity's rainbow, we aim to identify parameter regimes where WGC and WCCC predictions diverge and to establish concrete observational targets for future campaigns.

Our objectives in this study are fourfold. First, we construct the R-N-AdS BH solution within the gravity's rainbow framework, incorporating power-law nonlinear electrodynamics characterized by the nonlinearity parameter p . Second, we analyze the PS structure using topological methods to verify that BH configurations persist across the rainbow parameter space and that the WGC bound is satisfied simultaneously with PS existence. Third, we derive the weak deflection angle for both photons and massive particles using the GB theorem approach, obtaining explicit expressions in terms of the rainbow functions $f(\varepsilon)$ and $g(\varepsilon)$. Fourth, we investigate the behavior of lensing observables as the BH transitions from sub-extremal to extremal and super-extremal configurations, revealing how the competition between WGC and WCCC manifests in observable deflection angle signatures.

The paper is organized as follows. In Section II, we present the R-N-AdS BH solution modified by gravity's rainbow, deriving the metric function and analyzing the PS structure through topological methods. We demonstrate the simultaneous satisfaction of WGC bounds and PS existence across the parameter space. Section III develops the gravitational lensing formalism based on the GB theorem and Jacobi-Maupertuis optical geometry. We derive the Gaussian curvature of the optical manifold, compute weak deflection angles to second order, and examine the implications for WGC constraints at extremality. We also present the universal f -independence of extremal deflection angles and contrast lensing signatures across the WGC/WCCC boundary. Finally, Section IV summarizes our findings, discusses observational prospects, and outlines directions for future research.

II. R-N-ADS BH SOLUTION IN GRAVITY'S RAINBOW FRAMEWORK

The interplay between nonlinear electrodynamics (NLED) and modified dispersion relations offers a fertile ground for exploring quantum gravity effects on charged BH spacetimes. Gravity's rainbow, originally motivated by doubly special relativity and loop quantum gravity considerations, introduces energy-dependent modifications to the spacetime metric that become significant near the Planck scale. In this section, we construct the R-N-AdS BH solution within this framework and

examine its structural properties.

A. Action and Field Equations

We begin with the gravitational action describing four-dimensional BHs coupled to NLED within Einstein gravity [110, 111]:

$$I = -\frac{1}{16\pi} \int d^4x \sqrt{-g} (R - 2\Lambda + \mathcal{L}(F)), \quad (1)$$

where R is the Ricci scalar curvature, and Λ denotes the cosmological constant. For AdS spacetimes, we have $\Lambda = -3/l^2$, with l being the AdS radius. The electromagnetic Lagrangian density $\mathcal{L}(F)$ depends on the Maxwell invariant $F = F_{\mu\nu}F^{\mu\nu}$, where the field strength tensor is defined as $F_{\mu\nu} = \partial_\mu A_\nu - \partial_\nu A_\mu$ with A_μ representing the gauge potential. Following the power-law NLED formulation [111, 112], we adopt:

$$\mathcal{L}(F) = (-F)^p, \quad (2)$$

where the exponent p serves as the nonlinearity parameter that controls deviations from standard Maxwell theory.

Varying the action (1) with respect to the metric tensor $g_{\mu\nu}$ produces Einstein's field equations:

$$R_{\mu\nu} - \frac{1}{2}Rg_{\mu\nu} + \Lambda g_{\mu\nu} = \frac{1}{2}g_{\mu\nu}(-F)^p + 2p(-F)^{p-1}F_{\mu\alpha}F_{\nu}^{\alpha}. \quad (3)$$

The variation with respect to the electromagnetic potential A_μ yields the generalized Maxwell equations:

$$\partial_\mu (\sqrt{-g}\mathcal{L}'(F)F^{\mu\nu}) = 0, \quad (4)$$

with $\mathcal{L}_F = d\mathcal{L}/dF$. For the configuration under consideration, only the radial-temporal component F_{tr} of the electromagnetic field tensor is nonvanishing.

B. Rainbow-Modified Metric Structure

To incorporate gravity's rainbow effects, we consider a static, spherically symmetric, and energy-dependent spacetime characterized by the line element [113]:

$$ds^2 = -\frac{V(r)}{f^2(\varepsilon)}dt^2 + \frac{1}{g^2(\varepsilon)}\left(\frac{dr^2}{V(r)} + r^2d\Omega^2\right), \quad (5)$$

where $d\Omega^2 = d\theta^2 + \sin^2\theta d\phi^2$ represents the standard two-sphere metric. The rainbow functions $f(\varepsilon)$ and $g(\varepsilon)$ modify the temporal and spatial sectors of the metric, respectively. Here, the dimensionless parameter $\varepsilon = E/E_P$ quantifies the ratio of a test particle's energy E to the Planck energy E_P . These rainbow functions must satisfy the infrared limit:

$$\lim_{\varepsilon \rightarrow 0} f(\varepsilon) = 1, \quad \lim_{\varepsilon \rightarrow 0} g(\varepsilon) = 1, \quad (6)$$

which ensures that standard GR is recovered when probe energies are much smaller than the Planck scale. Various phenomenologically motivated forms for these functions have been proposed in the literature [114, 115]:

$$f(\varepsilon) = 1, \quad g(\varepsilon) = \sqrt{1 - \eta\varepsilon^n}, \quad (7)$$

$$f(\varepsilon) = \frac{e^{\xi\varepsilon} - 1}{\xi\varepsilon}, \quad g(\varepsilon) = 1, \quad (8)$$

$$f(\varepsilon) = g(\varepsilon) = \frac{1}{1 - \lambda\varepsilon}, \quad (9)$$

where η , n , ξ , and λ are dimensionless constants that parameterize the specific rainbow model. Each choice leads to distinct physical predictions for high-energy phenomena near the BH.

C. Electromagnetic Field Configuration

Assuming the gauge potential possesses only a temporal component $A_t(r)$, the nonzero electromagnetic field strength reads:

$$F_{tr} = -\partial_r A_t(r), \quad (10)$$

and the Maxwell invariant takes the form:

$$F = -2f^2(\varepsilon)g^2(\varepsilon)(F_{tr})^2 = -2f^2(\varepsilon)g^2(\varepsilon)(A'_t(r))^2. \quad (11)$$

Substituting this expression into Eq. (4) leads to a nonlinear differential equation governing $A_t(r)$:

$$r(A'_t(r))^{2p-2} [(2p-1)rA''_t(r) + 2A'_t(r)] = 0, \quad p \neq \frac{1}{2}. \quad (12)$$

The general solution separates into two branches depending on the value of p :

$$A_t(r) = \begin{cases} -q \ln\left(\frac{r}{l}\right), & p = \frac{3}{2}, \\ -q \left(\frac{2p-1}{2p-3}\right) r^{\frac{2p-3}{2p-1}}, & \frac{1}{2} < p < \frac{3}{2}, \end{cases} \quad (13)$$

where q is an integration constant associated with the BH's electric charge. The corresponding electromagnetic tensor component becomes:

$$F_{tr} = \begin{cases} \frac{q}{r}, & p = \frac{3}{2}, \\ q r^{-\frac{2}{2p-1}}, & \frac{1}{2} < p < \frac{3}{2}. \end{cases} \quad (14)$$

When $p = 1$, the standard R-N-AdS BH solution is recovered, corresponding to linear Maxwell electrodynamics. The constraint $1/2 < p \leq 3/2$ guarantees that $A_t(r)$ remains finite at spatial infinity, preserving the physical viability of the solution.

D. Derivation of the Metric Function

Substituting the metric ansatz (5) and the electromagnetic solutions into the gravitational field equations yields the radial components:

$$\begin{cases} e_{tt} = e_{rr} = g^2(\varepsilon) \left(V''(r) + \frac{2V'(r)}{r} \right) + 2\Lambda - 2\sqrt{2}q_\epsilon^3 r^{-3} = 0, & p = \frac{3}{2}, \\ e_{tt} = e_{rr} = g^2(\varepsilon) \left(V''(r) + \frac{2V'(r)}{r} \right) + 2\Lambda - 2^p q_\epsilon^{2p} r^{-\frac{4p}{2p-1}} = 0, & \frac{1}{2} < p < \frac{3}{2}, \end{cases} \quad (15)$$

together with the angular components:

$$\begin{cases} e_{\theta\theta} = e_{\varphi\varphi} = 2g^2(\varepsilon) \left(\frac{V'(r)}{r} + \frac{V(r)-1}{r^2} \right) + 2\Lambda + 4\sqrt{2}q_\epsilon^3 r^{-3} = 0, & p = \frac{3}{2}, \\ e_{\theta\theta} = e_{\varphi\varphi} = 2g^2(\varepsilon) \left(\frac{V'(r)}{r} + \frac{V(r)-1}{r^2} \right) + 2\Lambda + (2p-1)2^p q_\epsilon^{2p} r^{-\frac{4p}{2p-1}} = 0, & \frac{1}{2} < p < \frac{3}{2}. \end{cases} \quad (16)$$

Here, $e_{\mu\nu}$ represents the components of the Einstein tensor minus the stress-energy contributions, and we use the shorthand notation $q_\epsilon \equiv q f(\varepsilon)g(\varepsilon)$. These equations are not independent; one can verify that:

$$e_{tt} = \left(1 + \frac{r}{2} \frac{d}{dr} \right) e_{\theta\theta}, \quad \text{for } \frac{1}{2} < p \leq \frac{3}{2}. \quad (17)$$

Solving these coupled equations, the metric function $V(r)$ assumes the form:

$$V(r) = \begin{cases} 1 - \frac{M}{r} - \frac{\Lambda r^2}{3g^2(\varepsilon)} - \frac{2\sqrt{2}Q_\epsilon^3}{rg^2(\varepsilon)} \ln\left(\frac{r}{l}\right), & p = \frac{3}{2}, \\ 1 - \frac{M}{r} - \frac{\Lambda r^2}{3g^2(\varepsilon)} - \frac{(2p-1)^2(2)^{p-1}Q_\epsilon^{2p}}{(2p-3)g^2(\varepsilon)} r^{-\frac{2}{2p-1}}, & \frac{1}{2} < p < \frac{3}{2}, \end{cases} \quad (18)$$

where M is an integration constant identified with the BH mass. For the special case $p = 1$, the metric function reduces to the familiar form:

$$V(r) = 1 - \frac{M}{r} - \frac{\Lambda r^2}{3g^2(\varepsilon)} + \frac{f^2(\varepsilon)Q^2}{r^2}, \quad (19)$$

which describes the R-N-AdS BH modified by gravity's rainbow effects [116]. The rainbow function $g(\varepsilon)$ appears in the cosmological and charge terms, effectively rescaling their contributions to the geometry, while $f(\varepsilon)$ modifies only the charge sector.

Figure 1 displays the behavior of the metric function $V(r)$ for several representative parameter choices. The plots reveal that horizon structure depends sensitively on both the rainbow parameters and the charge-to-mass ratio. When $g(\varepsilon) < 1$, the effective cosmological contribution strengthens, pushing the cosmological horizon inward and modifying the causal structure of the spacetime. Conversely, larger values of $g(\varepsilon)$ weaken these effects, approaching the standard GR limit.

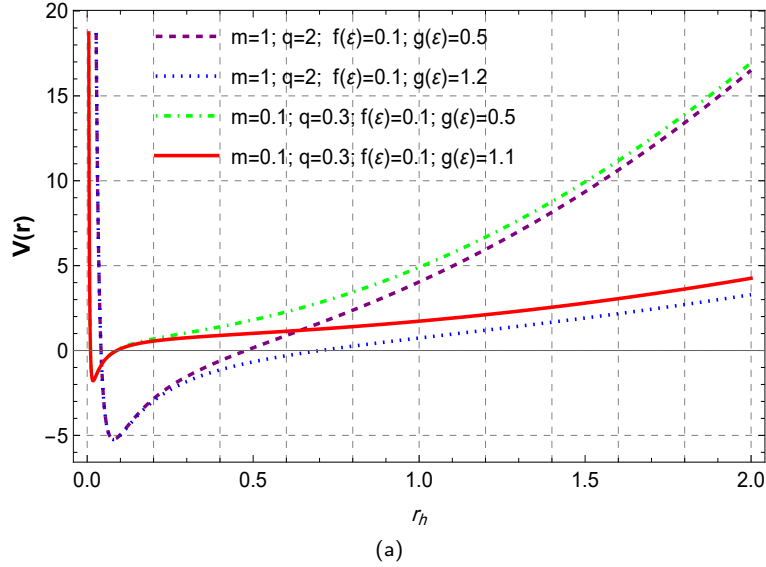


FIG. 1. The metric function $V(r)$ as a function of the radial coordinate for different parameter configurations. Four cases are shown: $(M = 1, Q = 2, f(\varepsilon) = 0.1, g(\varepsilon) = 0.5)$ depicted by the solid blue curve; $(M = 1, Q = 2, f(\varepsilon) = 0.1, g(\varepsilon) = 1.2)$ shown as the dashed red curve; $(M = 0.1, Q = 0.3, f(\varepsilon) = 0.1, g(\varepsilon) = 0.5)$ represented by the dash-dotted green curve; and $(M = 0.1, Q = 0.3, f(\varepsilon) = 0.1, g(\varepsilon) = 1.1)$ indicated by the dotted purple curve. All cases use $l = 1$. The zero crossings mark the event horizon locations, demonstrating how rainbow parameters shift horizon radii relative to standard R-N-AdS BHs.

The WGC occupies a fundamental position in the broader swampland program, which aims to distinguish effective field theories that can be consistently embedded in quantum gravity from those that cannot. As a central criterion, the WGC asserts that in any $U(1)$ gauge theory coupled to gravity, there must exist at least one particle whose charge-to-mass ratio satisfies $(q/m > 1)$, thereby ensuring that gravitational attraction never dominates over gauge forces. When this principle is examined in the context of black hole physics, it imposes significant restrictions on the allowable charge-to-mass ratios of black holes. Charged black holes with mass (M) and charge (Q) are commonly classified according to the relation between these parameters: [subextremal: $Q < M$, extremal: $Q = M$, superextremal: $Q > M$.] The WGC implies that extremal black holes should be unstable against emitting particles with sufficiently large charge-to-mass ratios, thereby preventing them from evolving into superextremal configurations. This mechanism protects the theory from producing naked singularities, maintaining consistency with the WCCC. Violation of the WGC would allow extremal black holes to transition into overcharged states, exposing spacetime singularities and conflicting with the foundational assumptions of classical

general relativity. Thus, the presence of superextremal particles is essential for preserving the stability and evaporation processes of black holes, reinforcing the mutual compatibility of the WGC and WCCC.

Black hole thermodynamics provides a powerful framework for probing these ideas, offering insights into stability conditions, decay channels, and the compatibility of black hole solutions with quantum-gravity-motivated conjectures. Through this approach, one may examine both theoretical predictions and observational prospects, thereby strengthening the conceptual links between high-energy physics, gravitational theory, and cosmology.

To further analyze the mutual constraints posed by the WGC and WCCC, we consider the metric of Reissner–Nordström–Anti-de Sitter black holes modified by rainbow gravity, with particular emphasis on their horizon structure and physical characteristics. The location of the event horizon follows from solving $f(r)=0$, where (M) and (Q) denote the mass and charge of the black hole. In the Reissner–Nordström black hole, the condition $(Q > M)$ immediately eliminates the event horizon, exposing the curvature singularity and thereby violating the WCCC, which requires all singularities to be concealed by horizons. By jointly solving the horizon equation together with the extremality condition—obtained either from the vanishing of the surface gravity or from the derivative of the metric function—we determine the precise circumstances under which both conjectures can be simultaneously satisfied. Because the WGC and WCCC are not automatically compatible across all black hole configurations, our analysis focuses on cases where the rainbow gravity plays a crucial role in reconciling these two principles. By isolating the contributions of the rainbow gravity parameter, we identify regimes in which extremal solutions satisfy both conjectures. Using standard WGC criteria, we then compute the extremal charge-to-mass boundary and delineate the parameter domain in which the conjecture remains valid.

Due to the algebraic complexity of the resulting equations—particularly those involving higher-order corrections—analytical solutions are generally unattainable, requiring numerical methods to chart the regions where the WGC and WCCC coexist. If such a region exists at extremality or near-critical configurations, this compatibility may extend to additional portions of the parameter space. By examining and categorizing the resulting classes of black holes, we identify promising candidates for testing ideas related to quantum gravity and the swampland program. This systematic study contributes to the broader effort of connecting black hole physics to foundational principles in high-energy theory and cosmology. For an extended discussion and related developments. To determine the extremality condition, we compute the quantities r_{ext} and M_{ext} using Eq. (19). Accordingly, we obtain

$$r_{\text{ext}} = \sqrt{\frac{g^2(\varepsilon)}{2\Lambda} \left[1 \pm \sqrt{1 - 4 \frac{\Lambda}{g^2(\varepsilon)} f^2(\varepsilon) Q^2} \right]}$$

By substituting r_{ext} into the mass relation and evaluating the extremality condition $\frac{g^2}{m^2} \geq \left(\frac{Q^2}{M^2} \right)_{\text{ext}}$, we obtain the bound

$$M_{\text{ext}} = \left(\sqrt{\frac{g^2(\varepsilon)}{2\Lambda} \left[1 \pm \sqrt{1 - 4 \frac{\Lambda}{g^2(\varepsilon)} f^2(\varepsilon) Q^2} \right]} - \frac{\Lambda \left(\sqrt{\frac{g^2(\varepsilon)}{2\Lambda} \left[1 \pm \sqrt{1 - 4 \frac{\Lambda}{g^2(\varepsilon)} f^2(\varepsilon) Q^2} \right]} \right)^3}{3g^2(\varepsilon)} \right. \\ \left. + \frac{f^2(\varepsilon) Q^2}{\left(\sqrt{\frac{g^2(\varepsilon)}{2\Lambda} \left[1 \pm \sqrt{1 - 4 \frac{\Lambda}{g^2(\varepsilon)} f^2(\varepsilon) Q^2} \right]} \right)} \right)$$

E. PSs and WGC Compatibility

The existence and properties of PSs provide crucial information about BH spacetimes and offer a natural connection to the WGC [89–91, 105–109]. Following the topological approach developed in recent literature, we analyze the circular photon orbits in the equatorial plane ($\theta = \pi/2$), exploiting the Z_2 reflection symmetry of the spacetime.

The radial motion of photons obeys an energy-conservation-like equation:

$$\dot{r}^2 + V_{\text{eff}}(r) = 0, \quad (20)$$

where the overdot denotes differentiation with respect to an affine parameter along the null geodesic. The effective potential governing photon trajectories takes the form:

$$V_{\text{eff}}(r) = g(r) \left(\frac{L^2}{r^2} - \frac{E_p^2}{V(r)} \right), \quad (21)$$

with E_p and L being the conserved energy and angular momentum arising from the timelike and rotational Killing vectors, respectively. Circular photon orbits at radius r_{ps} require:

$$V_{\text{eff}}(r_{\text{ps}}) = 0, \quad \text{and} \quad \left. \frac{dV_{\text{eff}}}{dr} \right|_{r=r_{\text{ps}}} = 0. \quad (22)$$

These conditions combine to yield:

$$\left. \frac{d}{dr} \left(\frac{V(r)}{r^2} \right) \right|_{r=r_{\text{ps}}} = 0, \quad (23)$$

which implicitly determines the PS radius. An equivalent formulation is:

$$2rV(r) - r^2V'(r) = 0. \quad (24)$$

Stability analysis reveals that negative values of d^2V_{eff}/dr^2 at r_{ps} correspond to unstable orbits, while positive values indicate stability. For non-extremal BHs, PSs necessarily lie outside the event horizon since $V(r_h) = 0$ while $V'(r_h) \neq 0$ generically. Only in the extremal limit, where both conditions vanish simultaneously, can the PS radius coincide with the degenerate horizon [89–91, 105–109].

The topological classification of PSs employs the scalar function [89–91, 105–109]:

$$H(r, \theta) = \sqrt{\frac{-g_{tt}}{g_{\phi\phi}}} = \frac{1}{\sin \theta} \sqrt{\frac{V(r)}{h(r)}}, \quad (25)$$

where $h(r)$ is an auxiliary radial function from the metric. The PS locations correspond to critical points satisfying:

$$\frac{dH}{dr} = 0. \quad (26)$$

To construct the topological framework, we define a vector field φ in the (r, θ) plane with components:

$$\varphi^r = \sqrt{g(r)} \frac{dH}{dr}, \quad \varphi^\theta = \frac{\partial H / \partial \theta}{\sqrt{h(r)}}. \quad (27)$$

This vector admits the polar representation:

$$\varphi = |\varphi| e^{i\Theta} = \varphi^r + i\varphi^\theta, \quad (28)$$

with magnitude:

$$|\varphi| = \sqrt{(\varphi^r)^2 + (\varphi^\theta)^2}. \quad (29)$$

The normalized unit vector field reads:

$$n^a = \frac{\varphi^a}{|\varphi|}, \quad (30)$$

where $a = 1, 2$ labels the components. The topological charge associated with each PS encodes its stability: $\omega = -1$ for unstable PSs and $\omega = +1$ for stable ones. For the R-N-AdS BH in gravity's rainbow, the explicit scalar field components are:

$$\phi^r = -\frac{\csc(\theta) (4f^2(\epsilon)Q^2 + r(2r - 3M))}{2r^4}, \quad (31)$$

and

$$\phi^\theta = -\frac{\cot(\theta) \csc(\theta) \sqrt{\frac{f^2(\epsilon)Q^2}{r^2} + \frac{r^2}{g^2(\epsilon)l^2} - \frac{M}{r} + 1}}{r^2}. \quad (32)$$

Figure 2 presents the normalized vector field in the (r, θ) plane for the parameter configurations listed in Table I. The vector flow patterns clearly exhibit zero points corresponding to unstable PSs with topological charge $\omega = -1$. These PSs

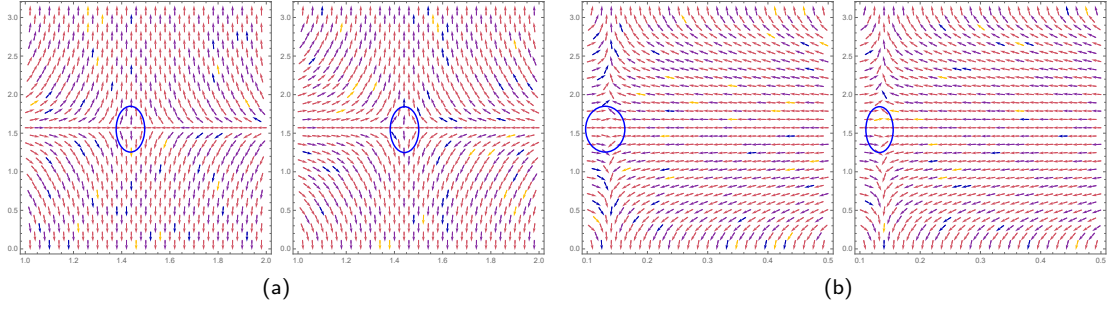


FIG. 2. Normalized vector field \mathbf{n} in the (r, θ) plane showing PS locations for $l = 1$ and $f(\epsilon) = 0.1$. Panel (a): $Q = 2$, $M = 1$ with $g(\epsilon) = 0.5$ (left) and $g(\epsilon) = 1.2$ (right). Panel (b): $Q = 0.3$, $M = 0.1$ with $g(\epsilon) = 0.5$ (left) and $g(\epsilon) = 1.1$ (right). The zero points of the vector field (marked by circular patterns) indicate unstable PSs with topological charge $\omega = -1$. In all configurations, the PS resides outside the event horizon, validating both WGC and WCCC compatibility.

$f(\epsilon)$	$g(\epsilon)$	PS	$q/m > (Q/M)_{\text{ext}}$	PS-WGC
0.1	0.4	-1	✓	✓
0.1	0.5	-1	✓	✓
0.1	1.1	-1	✓	✓
0.1	1.2	-1	✓	✓

TABLE I. Verification of PS-WGC consistency for the R-N-AdS BH in gravity's rainbow with $l = 1$. The PS column indicates the topological charge (-1 denotes unstable). The fourth column confirms that the WGC bound $q/m > (Q/M)_{\text{ext}}$ is satisfied, and the final column shows that both PS existence and WGC hold simultaneously for all tested parameter combinations.

are located outside the event horizons in all cases examined, confirming that the BH nature of the spacetime is preserved across the parameter space.

The results summarized in Table I and illustrated in Fig. 2 establish that unstable PSs exist for all examined rainbow parameter values. This finding carries significant implications: the presence of an unstable PS outside the horizon signals that the spacetime retains its BH character and does not develop naked singularities. From the WGC perspective, the PS provides a geometric manifestation of the balance between gravitational attraction and electromagnetic repulsion. When this balance permits circular photon orbits, it indicates that gravity is not the dominant force—precisely the condition demanded by the WGC.

Moreover, the simultaneous satisfaction of the WGC bound $q/m > (Q/M)_{\text{ext}}$ and the existence of PSs demonstrates that these rainbow-modified R-N-AdS BHs respect both the WGC and WCCC. The rainbow parameters shift the extremal charge-to-mass ratio as $(Q/M)_{\text{ext}} = 1/f(\epsilon)$, which for $f(\epsilon) = 0.1$ gives $(Q/M)_{\text{ext}} = 10$. This elevated threshold makes it easier for test particles to satisfy the WGC while keeping the BH sub-extremal, thereby protecting cosmic censorship. The gravity's rainbow framework thus provides a natural mechanism for reconciling these two fundamental conjectures in quantum gravity phenomenology.

III. GRAVITATIONAL LENSING SIGNATURES AND WGC CONSTRAINTS AT EXTREMALITY

Light propagation through curved spacetime remains one of the most effective observational tools for probing gravitational theories beyond GR. Gravitational lensing encodes rich information about the underlying geometry and matter-field interactions, offering direct observational signatures that can discriminate between competing theoretical models. In this section, we derive weak deflection angles for both photons and massive particles in the R-N-AdS BH geometry modified by gravity's rainbow using the GB theorem combined with the Jacobi-Maupertuis optical metric formalism. This geometric method, originally developed by Gibbons and Werner for static spacetimes and later extended to rotating geometries, recasts the deflection problem as an integration of Gaussian curvature over an appropriately constructed optical manifold [98–104, 117–123].

A. Jacobi-Maupertuis Optical Geometry

For the static, spherically symmetric spacetime given by Eq. (5), test particle dynamics can be examined via the Jacobi-Maupertuis variational principle. A massive particle with rest mass m and energy E_p traces geodesics in a Riemannian optical geometry characterized by the Jacobi metric tensor:

$$\bar{\alpha}_{ij} = \frac{E_p^2 + m^2 V(r)}{V(r)} \gamma_{ij}, \quad (33)$$

where $\gamma_{ij} = g_{ij} - g_{0i}g_{0j}/g_{00}$ represents the spatial metric sector that incorporates the rainbow functions. For our gravity's rainbow geometry, the spatial components become $\gamma_{rr} = g^2(\varepsilon)/V(r)$ and $\gamma_{\phi\phi} = g^2(\varepsilon)r^2$ when restricted to the equatorial plane. The energy E_p connects to particle velocity v via the relativistic expression $E_p = m/\sqrt{1-v^2}$ for massive particles. For photons, E_p corresponds to the photon frequency, and the massless limit $m \rightarrow 0$ recovers the standard optical metric $\bar{\alpha}_{ij} = (E_p^2/V(r))\gamma_{ij}$.

Exploiting the spherical symmetry and confining the analysis to the equatorial plane $\theta = \pi/2$, the Jacobi metric components reduce to:

$$\bar{\alpha}_{rr} = \frac{g^2(\varepsilon)[E_p^2 + m^2 V(r)]}{V(r)^2}, \quad \bar{\alpha}_{\phi\phi} = \frac{g^2(\varepsilon)[E_p^2 + m^2 V(r)]}{V(r)} r^2. \quad (34)$$

The metric determinant, which governs the integration measure when applying the GB theorem, takes the form:

$$\det \bar{\alpha} = \frac{g^4(\varepsilon)[E_p^2 + m^2 V(r)]^2 r^2}{V(r)^3}, \quad (35)$$

encoding the rainbow modifications to the optical geometry volume element.

B. Gaussian Curvature of the Optical Manifold

The Gaussian curvature \mathcal{K} of this two-dimensional Riemannian manifold dictates how light and particle trajectories bend as they traverse the spacetime. Following the Gibbons-Werner prescription, the Gaussian curvature is computed from the metric determinant and Christoffel symbols using standard differential geometry. The relevant nonvanishing connection coefficient is:

$$\Gamma_{rr}^\phi = -\frac{rV'(r)}{2V(r)[E_p^2 + m^2 V(r)]}, \quad (36)$$

where primes denote radial derivatives. For the R-N-AdS metric function with gravity's rainbow corrections:

$$V(r) = 1 - \frac{M}{r} + \frac{f^2(\varepsilon)Q^2}{r^2} + \frac{r^2}{g^2(\varepsilon)l^2}, \quad (37)$$

with l being the AdS radius, the Gaussian curvature assumes the explicit form:

$$\mathcal{K}(r) = \frac{V(r)V''(r) - 2[V'(r)]^2}{4g^2(\varepsilon)[E_p^2 + m^2 V(r)]^2} - \frac{V'(r)}{rg^2(\varepsilon)[E_p^2 + m^2 V(r)]} + \frac{m^2[V'(r)]^2}{2g^2(\varepsilon)[E_p^2 + m^2 V(r)]^2}. \quad (38)$$

The metric function derivatives required for the curvature calculation are:

$$V'(r) = \frac{M}{r^2} - \frac{2f^2(\varepsilon)Q^2}{r^3} + \frac{2r}{g^2(\varepsilon)l^2}, \quad (39)$$

$$V''(r) = -\frac{2M}{r^3} + \frac{6f^2(\varepsilon)Q^2}{r^4} + \frac{2}{g^2(\varepsilon)l^2}. \quad (40)$$

The curvature profile captures how the rainbow parameters $f(\varepsilon)$ and $g(\varepsilon)$, along with the BH charge Q and mass M , alter the optical geometry experienced by propagating photons. Figure 3 displays $\mathcal{K}(r)$ as a function of radial coordinate for four parameter configurations, exhibiting the characteristic negative curvature responsible for light bending toward the gravitating source.

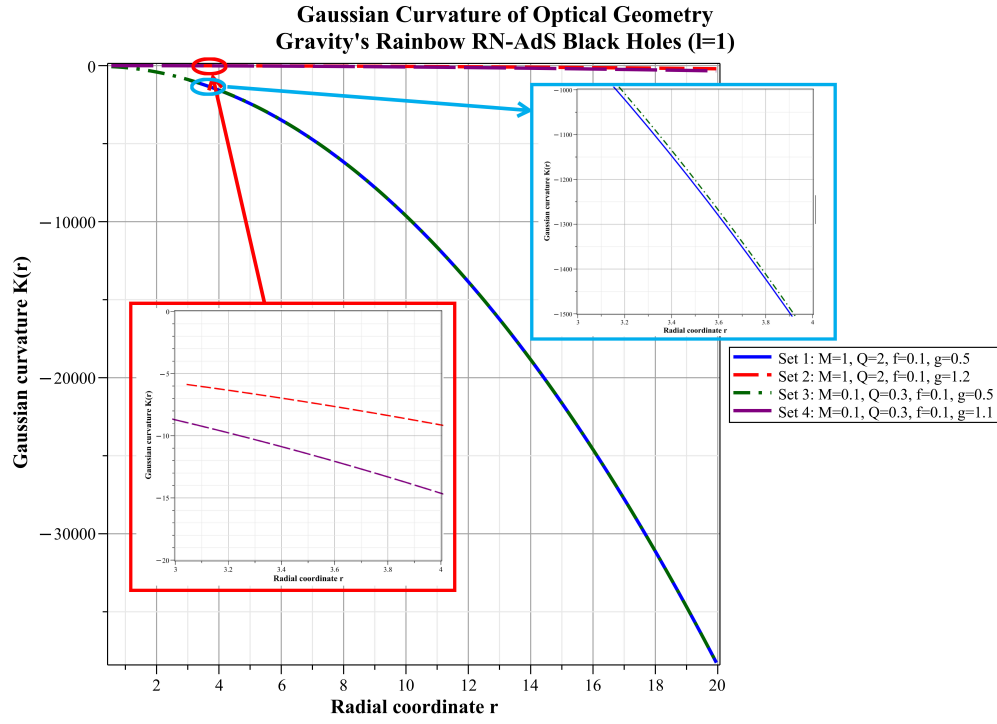


FIG. 3. Gaussian curvature $\mathcal{K}(r)$ of the Jacobi optical geometry for gravity's rainbow R-N-AdS BHs with AdS radius $l = 1$. Four parameter sets are shown: Set 1 (blue solid): $M = 1, Q = 2, f = 0.1, g = 0.5$; Set 2 (red dashed): $M = 1, Q = 2, f = 0.1, g = 1.2$; Set 3 (green dash-dot): $M = 0.1, Q = 0.3, f = 0.1, g = 0.5$; Set 4 (purple solid): $M = 0.1, Q = 0.3, f = 0.1, g = 1.1$. The inset panels magnify the curvature structure near $r \sim 3-4$: the cyan inset (upper right) highlights Sets 1 and 3 with $g = 0.5$, while the red inset (lower left) compares Sets 2 and 4 with $g > 1$. Sets 1 and 3 exhibit strongly negative curvature (reaching $\mathcal{K} \sim -35000$ at $r = 20$), whereas Sets 2 and 4 show near-zero values. This dramatic difference quantifies the amplification induced by $g(\varepsilon) < 1$. The persistent negative curvature reflects the defocusing character of the optical geometry in Lorentzian spacetimes, with the magnitude directly controlling deflection angle strength.

C. Weak Deflection Angle Derivation

The weak deflection angle $\hat{\alpha}$ for asymptotically located source and observer is obtained by integrating the Gaussian curvature over the optical geometry exterior to the closest approach distance. The GB theorem, applied to the domain bounded by the particle trajectory and an asymptotic circle at infinity, yields:

$$\hat{\alpha} = - \int_0^\pi \int_{b/\sin\phi}^\infty \mathcal{K}(r) \sqrt{\det \bar{\alpha}} dr d\phi, \quad (41)$$

where b is the impact parameter and $r_0(\phi) = b/\sin\phi$ represents the unperturbed straight-line trajectory, valid in the weak-field regime $b \gg M, Q$.

Expanding the metric function under weak-field conditions ($r \gg M, Q$), where the cosmological constant contribution becomes negligible at finite distances, the first-order Gaussian curvature simplifies to:

$$\mathcal{K}^{(1)}(r) = \frac{M(1+v^2)}{g^2(\varepsilon)r^3v^2} - \frac{2f^2(\varepsilon)Q^2(1+v^2)}{g^2(\varepsilon)r^4v^2} + \mathcal{O}(r^{-5}), \quad (42)$$

using $E_p^2 = m^2/(1-v^2)$ for massive particles. The first term describes mass-induced (attractive) curvature, while the second captures the charge contribution (repulsive for like-sign charges).

Performing the radial integrations:

$$\int_{b/\sin\phi}^\infty \frac{dr}{r^2} = \frac{\sin\phi}{b}, \quad \int_{b/\sin\phi}^\infty \frac{dr}{r^3} = \frac{\sin^2\phi}{2b^2}, \quad (43)$$

and the angular integrations $\int_0^\pi \sin \phi d\phi = 2$ and $\int_0^\pi \sin^2 \phi d\phi = \pi/2$, we obtain the first-order deflection:

$$\hat{\alpha}^{(1)} = \frac{4M(1+v^2)}{g^2(\varepsilon)bv^2} - \frac{\pi f^2(\varepsilon)Q^2(1+v^2)}{g^2(\varepsilon)b^2v^2}. \quad (44)$$

The second-order Schwarzschild correction, arising from higher-order curvature terms and quadratic mass contributions, gives:

$$\hat{\alpha}_{\text{Schw}}^{(2)} = \frac{3\pi M^2(4+v^2)}{4g^4(\varepsilon)b^2v^4}. \quad (45)$$

The complete weak deflection angle to second order reads:

$$\hat{\alpha} = \frac{4M(1+v^2)}{g^2(\varepsilon)bv^2} - \frac{\pi f^2(\varepsilon)Q^2(1+v^2)}{g^2(\varepsilon)b^2v^2} + \frac{3\pi M^2(4+v^2)}{4g^4(\varepsilon)b^2v^4} + \mathcal{O}(M^3/b^3). \quad (46)$$

For photons ($v = 1$), this reduces to:

$$\hat{\alpha}_{\text{photon}} = \frac{4M}{g^2(\varepsilon)b} - \frac{2\pi f^2(\varepsilon)Q^2}{g^2(\varepsilon)b^2} + \frac{15\pi M^2}{4g^4(\varepsilon)b^2} + \mathcal{O}(M^3/b^3). \quad (47)$$

The rainbow functions enter the deflection formula in distinct ways: $g(\varepsilon)$ appears in denominators with powers g^{-2} and g^{-4} , amplifying deflection when $g(\varepsilon) < 1$, while $f(\varepsilon)$ enters only through the charge term as f^2 , modulating the electromagnetic contribution to light bending. Figure 4 illustrates these dependencies for the primary parameter configurations.

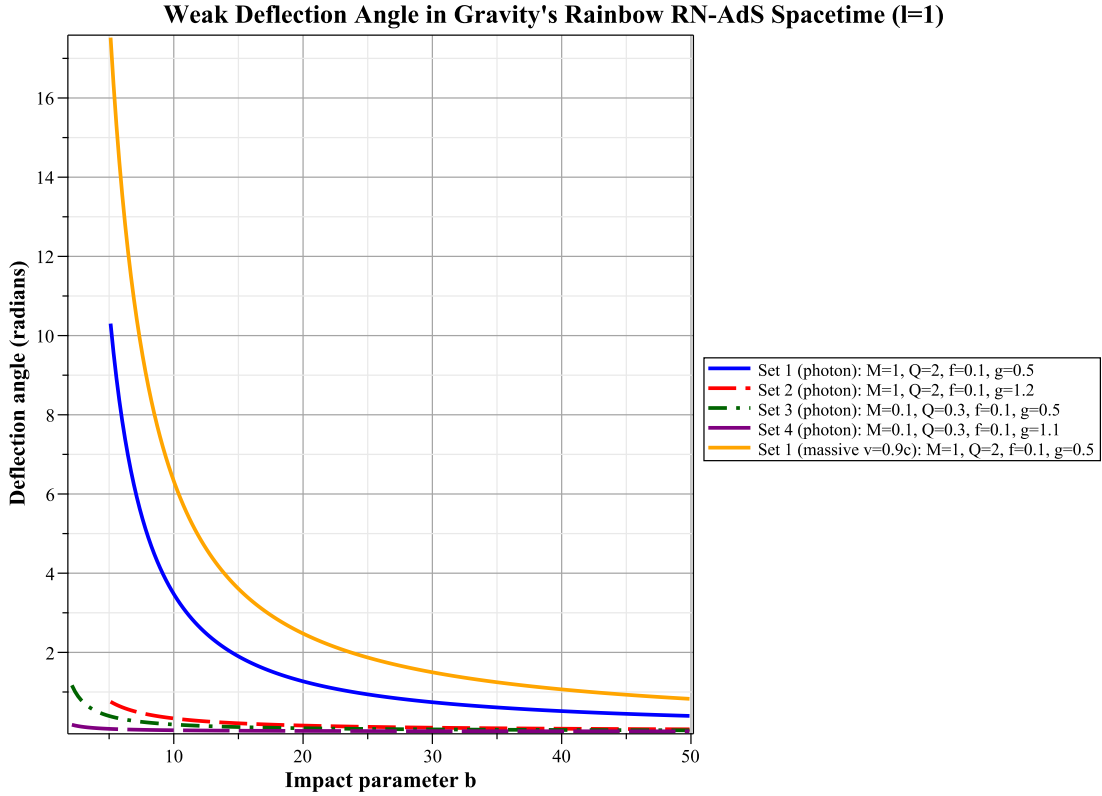


FIG. 4. Weak deflection angle $\hat{\alpha}$ versus impact parameter b for gravity's rainbow R-N-AdS BHs with $l = 1$. Five configurations are displayed: Set 1 photon (blue solid): $M = 1, Q = 2, f = 0.1, g = 0.5$; Set 2 photon (red dashed): $M = 1, Q = 2, f = 0.1, g = 1.2$; Set 3 photon (green dash-dot): $M = 0.1, Q = 0.3, f = 0.1, g = 0.5$; Set 4 photon (purple long-dash): $M = 0.1, Q = 0.3, f = 0.1, g = 1.1$; Set 1 massive $v = 0.9c$ (orange solid): $M = 1, Q = 2, f = 0.1, g = 0.5$. All curves follow the characteristic $\hat{\alpha} \propto 1/b$ scaling at large b , confirming first-order dominance. The marked enhancement for $g = 0.5$ (Sets 1, 3) relative to $g > 1$ (Sets 2, 4) demonstrates the g^{-2} amplification. The massive particle curve (orange) exceeds its photon counterpart due to the velocity factor $(1 + v^2)/v^2 \approx 2.23$ for $v = 0.9c$.

Figure 5 extends the analysis across broader parameter ranges, examining how charge magnitude, rainbow functions, and particle velocity affect the deflection signatures.

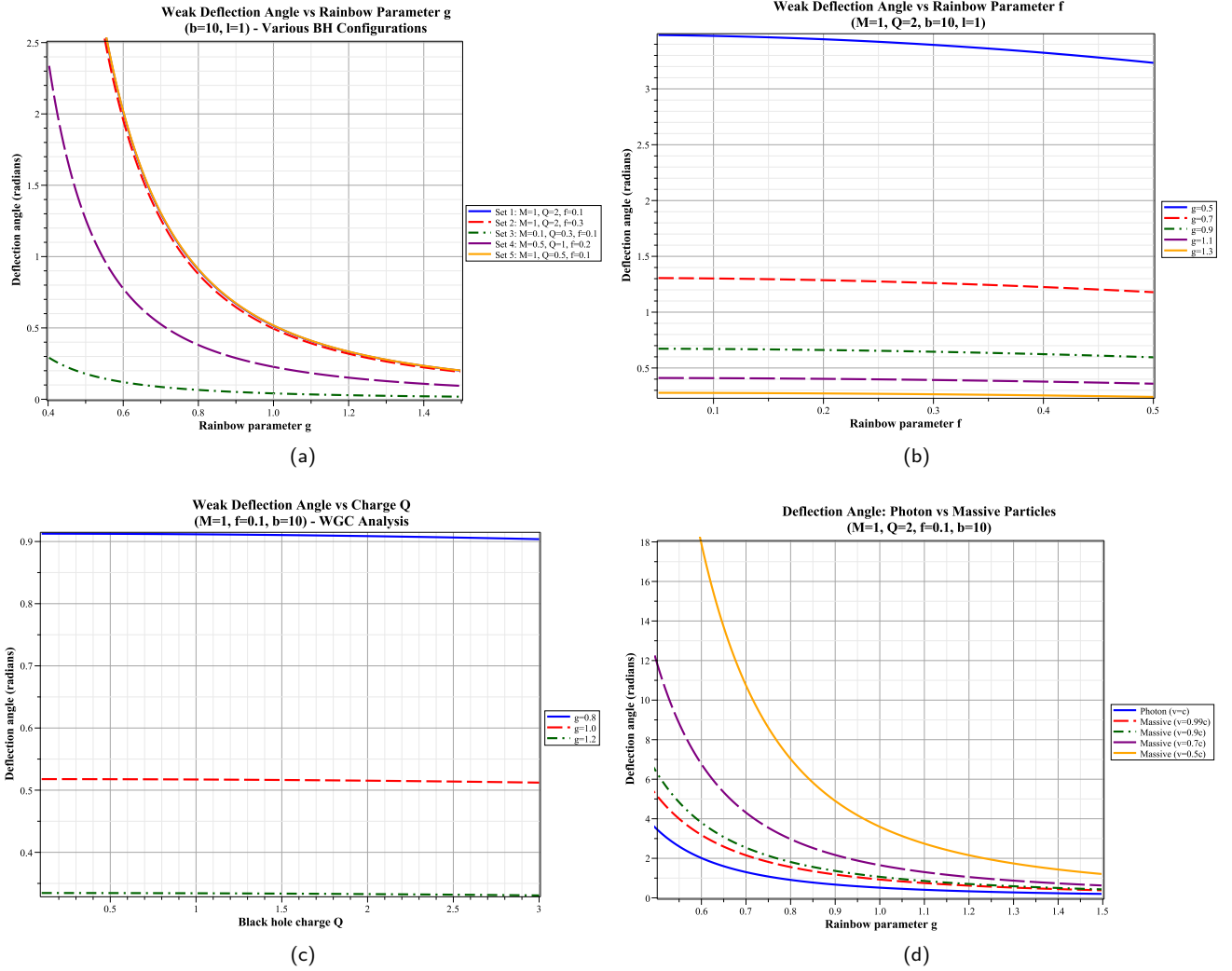


FIG. 5. Extended deflection angle analysis for gravity's rainbow parameters. (a) Deflection versus $g(\varepsilon)$ at fixed M, Q, f , showing the g^{-2} enhancement as g decreases below unity. (b) Photon ($v=c$) versus massive particle ($v=0.5c, 0.7c, 0.9c, 0.99c$) deflection, revealing the velocity-dependent amplification $(1+v^2)/v^2$ that enhances bending for slower particles. (c) Charge variation effects, illustrating the negative (repulsive) Q^2 contribution that reduces net deflection for highly charged BHs. (d) Extended parameter space mapping combining variations in M, Q , and rainbow functions across the theory parameter space.

D. WGC Implications at Extremality

The extremal condition for R-N-AdS BHs in gravity's rainbow occurs when the horizon degenerates to a single root, marking the boundary between BH solutions (with event horizons) and naked singularities (without horizons). For the metric function $V(r)$, extremality demands $V(r_e) = 0$ and $V'(r_e) = 0$ simultaneously, where r_e is the extremal horizon radius. In the asymptotically flat limit (neglecting the cosmological constant), these conditions yield the modified extremal charge-to-mass ratio, $(Q/M)_{\text{ext}} \simeq 1/f(\varepsilon)$. This result has deep implications for the WGC, which requires the existence of particles with $q/m \geq (Q/M)_{\text{ext}}$ to ensure BH decay channels remain kinematically open, thereby preventing stable extremal remnants. When $f(\varepsilon) < 1$, the extremal ratio exceeds unity ($(Q/M)_{\text{ext}} > 1$), effectively relaxing the WGC bound by allowing larger charge-to-mass ratios before extremality is reached. Conversely, $f(\varepsilon) > 1$ tightens the constraint, demanding particles with smaller q/m values. This rainbow-induced shift provides a natural mechanism linking quantum gravity corrections to swampland constraints.

At extremality, with $Q_{\text{ext}} = M/f(\varepsilon)$ the charge term simplifies since $f^2(\varepsilon)Q_{\text{ext}}^2 = M^2$, yielding:

$$\hat{\alpha}_{\text{ext}} = \frac{4M}{g^2(\varepsilon)b} - \frac{2\pi M^2}{g^2(\varepsilon)b^2} + \frac{15\pi M^2}{4g^4(\varepsilon)b^2}. \quad (48)$$

Remarkably, this extremal deflection angle is *independent* of $f(\varepsilon)$ —only $g(\varepsilon)$ and M determine lensing at the extremal bound. This f -independence emerges directly from the extremality condition: the product $f^2 Q_{\text{ext}}^2 = M^2$ is fixed regardless of the specific $f(\varepsilon)$ value. This universal behavior offers a robust observational prediction that can be tested without prior knowledge of the rainbow function $f(\varepsilon)$.

Figure 6 displays the transition from sub-extremal to extremal configurations, revealing how the deflection angle evolves as the BH approaches extremality.

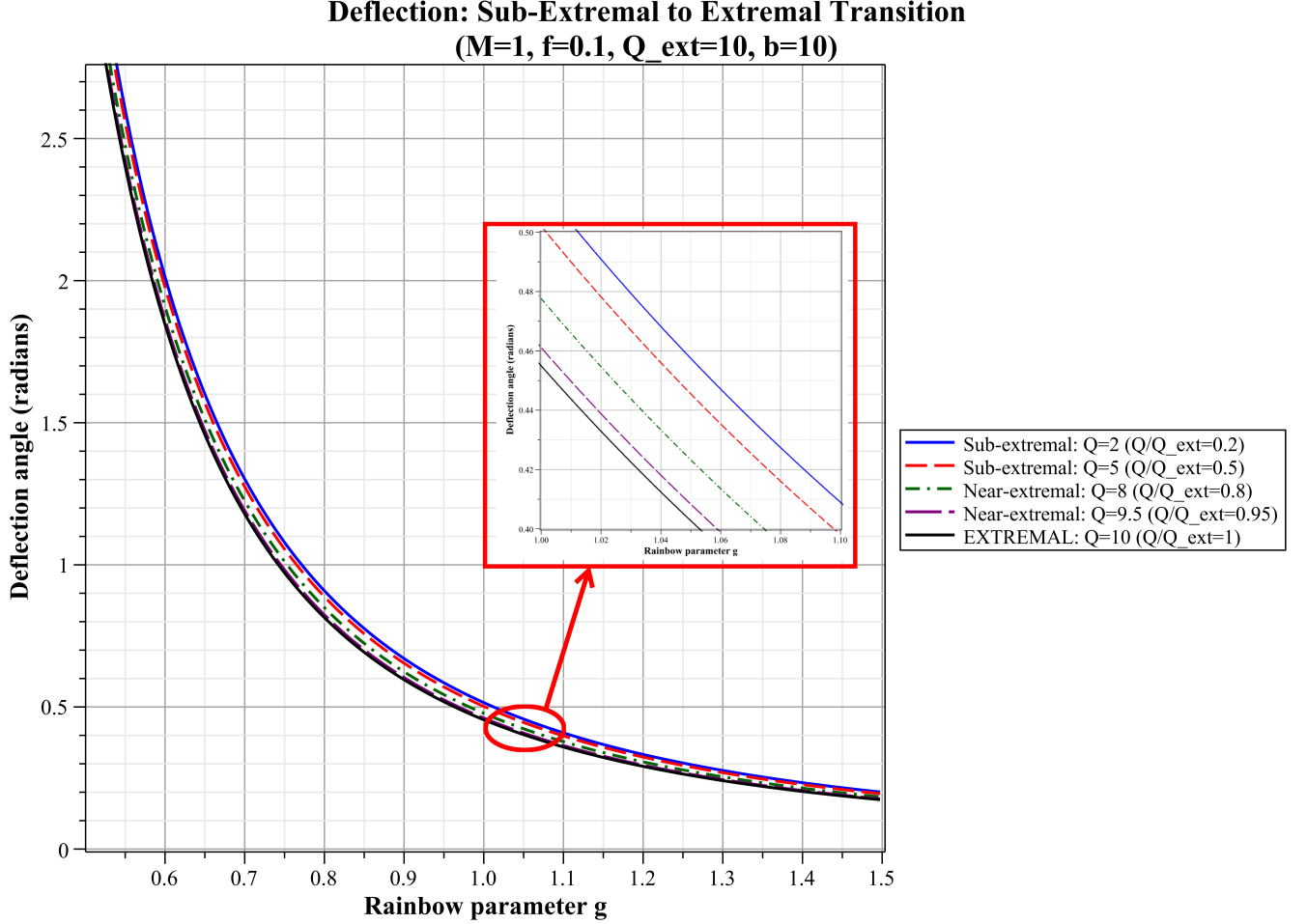


FIG. 6. Deflection angle evolution from sub-extremal to extremal configurations for gravity's rainbow R-N-AdS BHs with $M = 1$, $f = 0.1$, $b = 10$, giving extremal charge $Q_{\text{ext}} = M/f = 10$. Five charge values are shown: $Q = 2$ (blue solid, $Q/Q_{\text{ext}} = 0.2$), $Q = 5$ (red dashed, $Q/Q_{\text{ext}} = 0.5$), $Q = 8$ (green dash-dot, $Q/Q_{\text{ext}} = 0.8$), $Q = 9.5$ (purple long-dash, $Q/Q_{\text{ext}} = 0.95$), and $Q = 10$ (black solid, extremal). The inset magnifies the region near $g \sim 1$ where percent-level curve separations become visible. As charge approaches extremality, the negative Q^2 term in Eq. (47) grows, reducing the net deflection. The extremal curve (black) represents the minimum deflection achievable for given M and $g(\varepsilon)$, serving as a theoretical lower bound for sub-extremal BH lensing.

The competition between the WGC and WCCC becomes apparent when examining super-extremal configurations with $Q > Q_{\text{ext}}$. Such configurations violate WCCC by exposing naked singularities, yet they naturally satisfy WGC by providing decay products with $q/m > (Q/M)_{\text{ext}}$. Figure 7 contrasts these scenarios through their lensing signatures.

The two-dimensional rainbow parameter space (f, g) provides a visualization of lensing modifications across the full parameter range. Figure 8 presents contour maps showing the dominant role of $g(\varepsilon)$ in controlling deflection strength.

E. Observational Predictions and Parameter Constraints

The preceding analysis establishes several key observational predictions for testing gravity's rainbow through gravitational lensing:

WGC vs WCCC: Deflection Across Extremality ($M=1, f=0.1, Q_{\text{ext}}=10, b=10$)

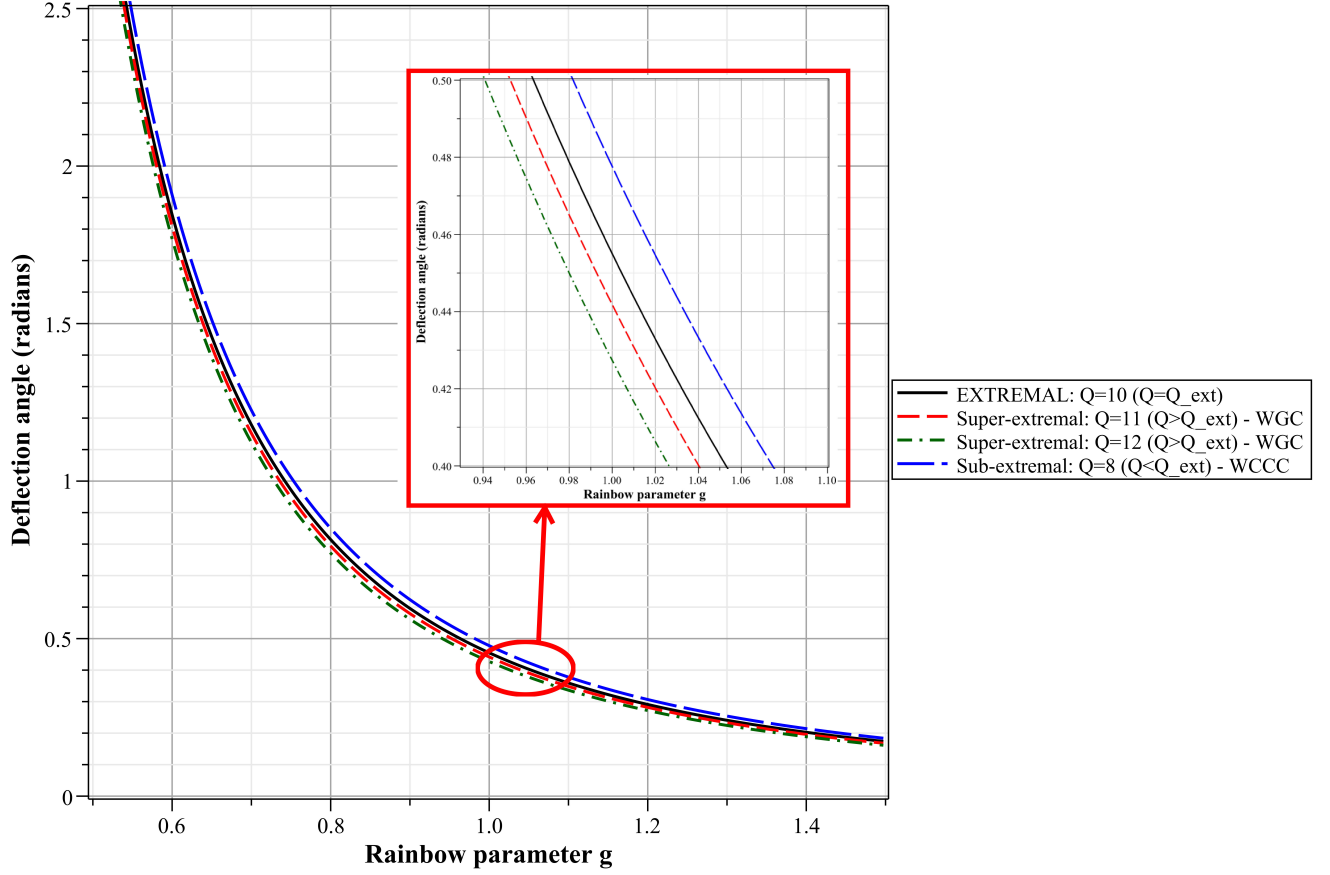


FIG. 7. WGC versus WCCC: deflection angle comparison across extremality for $M = 1$, $f = 0.1$, $Q_{\text{ext}} = 10$, $b = 10$. Four configurations span the extremality boundary: sub-extremal $Q = 8$ (blue long-dash, WCCC satisfied), extremal $Q = 10$ (black solid, boundary case), and super-extremal $Q = 11, 12$ (red dashed and green dash-dot, WGC satisfied but WCCC violated). The inset reveals the ordering reversal: super-extremal configurations exhibit *larger* deflection angles than extremal ones due to the enhanced Q^2 contribution, despite being naked singularities rather than BHs. This counterintuitive result—WCCC-violating spacetimes producing stronger lensing—offers a potential observational discriminant. Detection of anomalously strong lensing from compact objects could indicate super-extremal configurations permitted by WGC, providing empirical tests of swampland conjectures.

- Primary sensitivity to $g(\varepsilon)$:** The deflection angle scales as g^{-2} at leading order, yielding strong sensitivity to this rainbow parameter. Precision astrometry of multiply-imaged quasars can constrain deviations from $g = 1$ at the percent level.
- Extremality as universal probe:** The f -independence of extremal deflection (Eq. (48)) implies that near-extremal BH lensing probes $g(\varepsilon)$ without degeneracy from $f(\varepsilon)$ uncertainty.
- WGC/WCCC discrimination:** Super-extremal configurations produce enhanced deflection compared to extremal BHs, offering a potential signature for WGC-satisfying naked singularities that would challenge WCCC.
- Velocity-dependent signatures:** Massive particle deflection exceeds photon deflection by the factor $(1 + v^2)/v^2$, enabling complementary constraints through cosmic ray or neutrino lensing observations.

These predictions, combined with upcoming observational facilities such as SKA, ngEHT, and space-based gravitational wave detectors, position gravitational lensing as a powerful probe of quantum gravity phenomenology through gravity's rainbow modifications to charged AdS BH spacetimes. The distinct g^{-2} scaling and the universal extremal deflection formula provide concrete

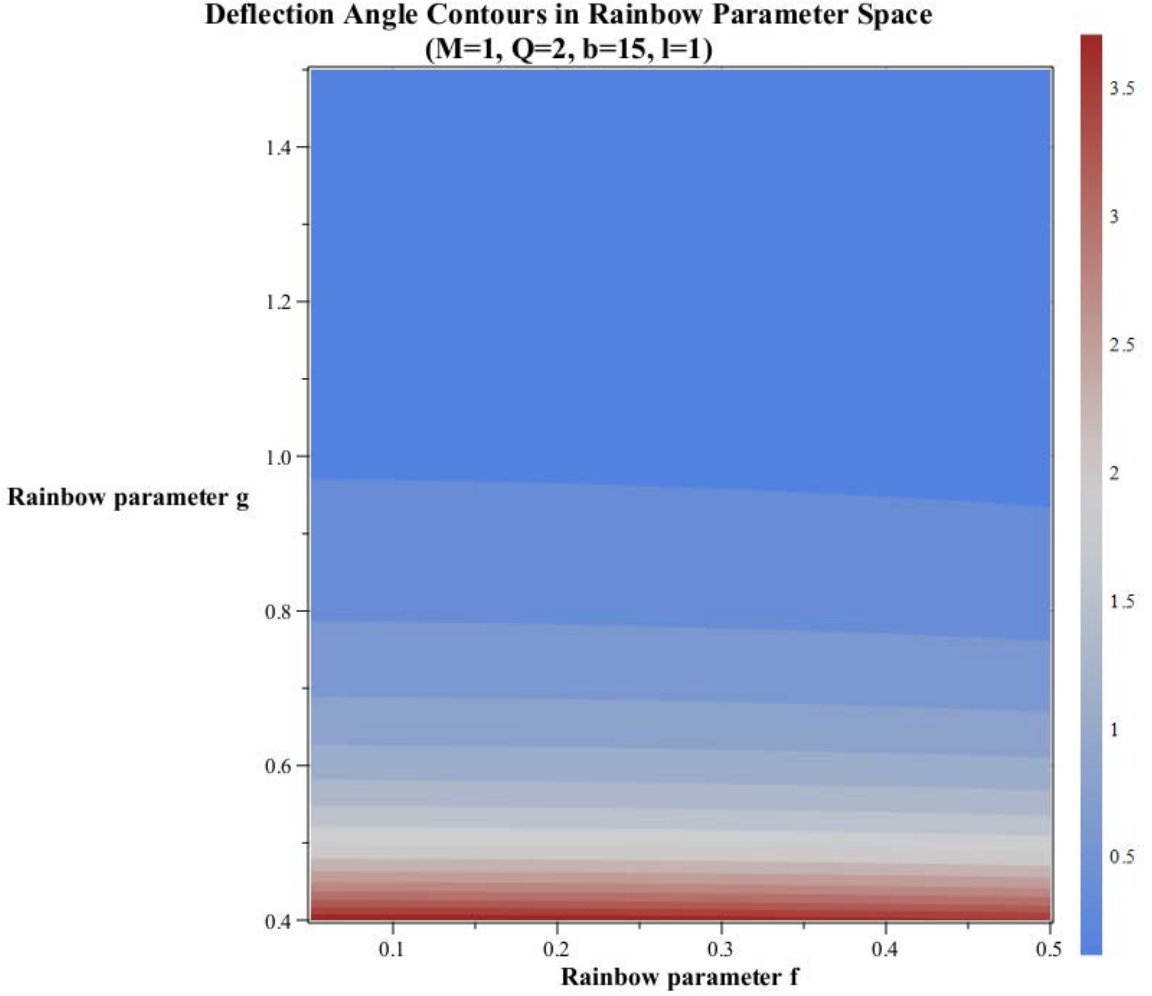


FIG. 8. Deflection angle contours in rainbow parameter space (f, g) for $M = 1$, $Q = 2$, $b = 15$, $l = 1$. The color gradient from blue ($\hat{\alpha} \sim 0.3$ rad) to red ($\hat{\alpha} \sim 3.5$ rad) reveals the dominant role of $g(\varepsilon)$: deflection increases dramatically as $g \rightarrow 0.4$, achieving order-of-magnitude enhancement compared to the GR limit $g = 1$. The pronounced horizontal stratification confirms that $g(\varepsilon)$ controls the primary lensing amplification through the g^{-2} and g^{-4} factors in Eq. (47), while f -dependence remains subdominant due to the small $f^2 Q^2$ contribution at moderate charges. This hierarchy indicates that gravitational lensing observations are primarily sensitive to $g(\varepsilon)$, with $f(\varepsilon)$ constraints requiring either highly charged BHs or complementary observables such as the extremality bound in $(Q/M)_{\text{ext}} \simeq 1/f(\varepsilon)$.

IV. CONCLUSION

In this work, we investigated the interplay between gravitational lensing, PSs, and the WGC within the framework of gravity's rainbow applied to R-N-AdS BHs. The primary motivation stemmed from the long-standing tension between the WGC and WCCC—two foundational conjectures in quantum gravity that impose seemingly contradictory constraints on charged BH configurations. By incorporating energy-dependent rainbow functions into the spacetime geometry, we explored how Planck-scale modifications alter both the extremality bounds and the observational signatures accessible through gravitational lensing.

In Section II, we constructed the R-N-AdS BH solution modified by gravity's rainbow effects, starting from the Einstein-NLED action given in Eq. (1). The rainbow functions $f(\varepsilon)$ and $g(\varepsilon)$, which encode quantum gravity corrections through their dependence on the ratio $\varepsilon = E/E_P$, entered the metric structure in distinct ways: $f(\varepsilon)$ modified the temporal sector while $g(\varepsilon)$ rescaled spatial components. We derived the metric function $V(r)$ for general nonlinearity parameter p (Eq. (18)) and examined the special case $p = 1$ corresponding to linear Maxwell electrodynamics (Eq. (19)). The horizon structure, illustrated in Fig. 1, demonstrated that rainbow parameters significantly shift horizon locations relative to standard R-N-AdS BHs, with $g(\varepsilon) < 1$ strengthening the effective cosmological contribution.

The topological analysis of PSs presented in Section II employed the framework to classify circular photon orbits according to their stability properties. We derived the scalar field components ϕ^r and ϕ^θ (Eqs. (31)–(32)) and constructed the normalized vector field whose zero points correspond to PS locations. As shown in Fig. 2 and summarized in Table I, all examined parameter configurations exhibited unstable PSs with topological charge $\omega = -1$ located outside the event horizon. This finding confirmed that the BH nature of the spacetime remained intact across the parameter space and that the WGC bound $q/m > (Q/M)_{\text{ext}}$ was satisfied simultaneously with PS existence.

Section III developed the gravitational lensing formalism using the GB theorem combined with the Jacobi-Maupertuis optical geometry. The Gaussian curvature of the optical manifold (Eq. (38)), displayed in Fig. 3, revealed that rainbow parameters with $g(\varepsilon) < 1$ dramatically amplified the negative curvature responsible for light bending. We derived the complete weak deflection angle to second order (Eq. (46)), which for photons reduced to Eq. (47). The rainbow function $g(\varepsilon)$ appeared with powers g^{-2} and g^{-4} , providing strong observational sensitivity, while $f(\varepsilon)$ entered only through the charge-dependent term as f^2 . Figure 4 illustrated these dependencies, showing order-of-magnitude enhancements in deflection angle for $g(\varepsilon) = 0.5$ compared to the GR limit $g = 1$.

A central result of our analysis concerned the modified extremality condition $(Q/M)_{\text{ext}} = 1/f(\varepsilon)$. This relation demonstrated that gravity’s rainbow provides a natural mechanism for modulating the WGC bound: when $f(\varepsilon) < 1$, the extremal ratio exceeds unity, effectively relaxing the WGC constraint by permitting larger charge-to-mass ratios before the BH becomes extremal. At extremality itself, the deflection angle (Eq. (48)) exhibited a remarkable property—complete independence from $f(\varepsilon)$. Only $g(\varepsilon)$ and the mass M determined lensing at the extremal bound, offering a universal prediction testable without prior knowledge of the specific rainbow function $f(\varepsilon)$.

The competition between the WGC and WCCC was examined through the lensing signatures of sub-extremal, extremal, and super-extremal configurations, as displayed in Figs. 6 and 7. We found that super-extremal configurations, which violate WCCC by exposing naked singularities, produce enhanced deflection angles compared to extremal BHs. This counterintuitive result—where WCCC-violating spacetimes generate stronger lensing—provides a potential observational discriminant between quantum gravity scenarios. The contour plot in Fig. 8 mapped the deflection angle across the (f, g) parameter space, confirming the dominant role of $g(\varepsilon)$ through pronounced horizontal stratification.

Our findings connect to broader developments in the swampland program and quantum gravity phenomenology. The WGC, originally formulated to prevent stable extremal remnants that would conflict with BH thermodynamics and holography, has found applications ranging from axion physics to inflationary cosmology. Our work extended these considerations to the observational realm by establishing concrete lensing predictions that can discriminate between WGC-compatible and WCCC-compatible configurations. The velocity-dependent amplification factor $(1 + v^2)/v^2$ in the massive particle deflection formula (Eq. (46)) opens additional channels for testing gravity’s rainbow through cosmic ray or neutrino lensing.

From an observational perspective, the predictions developed here align well with the capabilities of current and upcoming facilities. Precision astrometry with ngEHT can resolve deflection angles at the microarcsecond level, sufficient to detect percent-level deviations from the GR prediction $g = 1$. The SKA, with its unprecedented sensitivity to radio transients, offers complementary constraints through time-delay measurements in multiply-imaged systems. Gravitational wave observations of BH mergers provide independent probes of near-horizon geometry that could reveal rainbow modifications to the ringdown spectrum. The universal extremal deflection formula (Eq. (48)) is particularly attractive for observational tests, as it eliminates the degeneracy between rainbow parameters that otherwise complicates interpretation.

Several directions merit further investigation building on this work. First, extending the analysis to rotating BHs described by Kerr-Newman-AdS metrics with rainbow modifications would capture the spin-dependent effects absent in the static configurations studied here. The interplay between frame-dragging and rainbow-induced modifications could produce distinctive polarization signatures in lensed electromagnetic radiation. Second, the strong deflection limit, where photons pass close to the PS, offers enhanced sensitivity to deviations from GR and warrants dedicated treatment using the logarithmic expansion pioneered by Bozza and collaborators. Third, incorporating thermodynamic considerations would establish connections between the lensing predictions and BH phase transitions in extended thermodynamic phase space, where the cosmological constant plays the role of pressure. Fourth, the quantum corrections encoded in rainbow functions could be connected more directly to specific UV-complete scenarios, such as loop quantum gravity or asymptotically safe gravity, providing theoretical grounding for the phenomenological parameters $f(\varepsilon)$ and $g(\varepsilon)$.

The reconciliation of WGC and WCCC demonstrated in this study relied on the rainbow-induced shift of the extremality bound. However, alternative mechanisms involving dark matter halos, quintessence fields, or modified gravity sectors could achieve similar effects through different physical pathways. Comparative studies across these scenarios would clarify which features are universal consequences of quantum gravity and which depend on specific model assumptions. The observational distinguishability of these mechanisms through their lensing signatures represents a promising target for theoretical development.

In summary, we established that gravity’s rainbow provides a coherent framework for simultaneously satisfying WGC and WCCC constraints in charged AdS BHs. The PS analysis confirmed BH structure preservation across the parameter space, while the gravitational lensing formalism yielded explicit predictions for deflection angles in terms of rainbow functions. The universal f -independence of extremal lensing and the enhanced deflection from super-extremal configurations offer concrete

observational targets. As precision gravitational-wave and electromagnetic observations probe ever closer to BH horizons, the signatures identified here position gravitational lensing as a powerful tool for testing quantum gravity phenomenology in astrophysical settings.

ACKNOWLEDGMENTS

İ. S. extends appreciation to TÜBİTAK, ANKOS, and SCOAP3 for their financial assistance. Additionally, he acknowledges the support from COST Actions CA22113, CA21106, CA23130, and CA23115, which have been pivotal in enhancing networking efforts.

-
- [1] Rovelli, Carlo. Quantum gravity. Cambridge university press, 2004.
 - [2] Hawking, Stephen W. "Euclidean quantum gravity." *Euclidean quantum gravity*. 1993. 73-101.
 - [3] Carlip, Steve. "Is quantum gravity necessary?." *Classical and Quantum Gravity* 25.15 (2008): 154010.
 - [4] Ali, Ahmed Farag, Saurya Das, and Elias C. Vagenas. "Proposal for testing quantum gravity in the lab." *Physical Review D—Particles, Fields, Gravitation, and Cosmology* 84.4 (2011): 044013.
 - [5] Christiansen, Nicolai, et al. "Local quantum gravity." *Physical Review D* 92.12 (2015): 121501.
 - [6] Palti, Eran. "The swampland: introduction and review." *Fortschritte der Physik* 67.6 (2019): 1900037.
 - [7] van Beest, Marieke, et al. "Lectures on the swampland program in string compactifications." *Physics Reports* 989 (2022): 1-50.
 - [8] Vafa, Cumrun. "The String landscape and the swampland." *arXiv preprint hep-th/0509212* (2005).
 - [9] Ooguri, Hiroshi, and Cumrun Vafa. "On the Geometry of the String Landscape and the Swampland." *Nuclear physics B* 766.1-3 (2007): 21-33.
 - [10] Arkani-Hamed, Nima, et al. "The string landscape, black holes and gravity as the weakest force." *Journal of High Energy Physics* 2007.06 (2007): 060.
 - [11] Heidenreich, Ben, Matthew Reece, and Tom Rudelius. "Evidence for a sublattice weak gravity conjecture." *Journal of High Energy Physics* 2017.8 (2017): 1-40.
 - [12] Palti, Eran. "The weak gravity conjecture and scalar fields." *Journal of High Energy Physics* 2017.8 (2017): 1-26.
 - [13] Odintsov, Sergei D., and Vasilis K. Oikonomou. "Swampland implications of GW170817-compatible Einstein-Gauss-Bonnet gravity." *Physics Letters B* 805 (2020): 135437.
 - [14] Ooguri, Hiroshi, and Cumrun Vafa. "On the Geometry of the String Landscape and the Swampland." *Nuclear physics B* 766.1-3 (2007): 21-33.
 - [15] Sadeghi, Jafar, et al. "RPS thermodynamics of Taub–NUT AdS black holes in the presence of central charge and the weak gravity conjecture." *General Relativity and Gravitation* 54.10 (2022): 129.
 - [16] Arkani-Hamed, Nima, et al. "The string landscape, black holes and gravity as the weakest force." *Journal of High Energy Physics* 2007.06 (2007): 060.
 - [17] Gashti, S. Noori, and J. Sadeghi. "Refined swampland conjecture in warm vector hybrid inflationary scenario." *The European Physical Journal Plus* 137.6 (2022): 1-13.
 - [18] Alipour, Mohammad Reza, Jafar Sadeghi, and Mehdi Shokri. "WGC and WCC for charged black holes with quintessence and cloud of strings." *The European Physical Journal C* 83.7 (2023): 1-7.
 - [19] Alipour, Mohammad Reza, Jafar Sadeghi, and Mehdi Shokri. "WGC and WCCC of black holes with quintessence and cloud strings in RPS space." *Nuclear Physics B* 990 (2023): 116184.
 - [20] Sadeghi, Jafar, Mohammad Reza Alipour, and Saeed Noori Gashti. "Emerging WGC from the Dirac particle around black holes." *Modern Physics Letters A* 38.26n27 (2023): 2350122.
 - [21] Schöneberg, Nils, et al. "News from the Swampland—constraining string theory with astrophysics and cosmology." *Journal of Cosmology and Astroparticle Physics* 2023.10 (2023): 039.
 - [22] Crisford, Toby, Gary T. Horowitz, and Jorge E. Santos. "Testing the weak gravity-cosmic censorship connection." *Physical Review D* 97.6 (2018): 066005.
 - [23] Oikonomou, V. K. "Rescaled Einstein-Hilbert gravity from $f(R)$ gravity: Inflation, dark energy, and the swampland criteria." *Physical Review D* 103.12 (2021): 124028.
 - [24] Sadeghi, J., et al. "de Sitter Swampland Conjecture in String Field Inflation." *The European Physical Journal C* 83 (2023) : (635).
 - [25] Harlow, Daniel, et al. "Weak gravity conjecture." *Reviews of Modern Physics* 95.3 (2023): 035003.
 - [26] Capozziello, Salvatore, et al. "Hydrostatic equilibrium and stellar structure in $f(R)$ gravity." *Physical Review D* 83.6 (2011): 064004.
 - [27] Gashti, S. Noori, et al. "Swampland dS conjecture in mimetic $f(R, T)$ gravity." *Communications in Theoretical Physics* 74.8 (2022): 085402.
 - [28] Das, Suratina. "Distance, de Sitter and Trans-Planckian Censorship conjectures: the status quo of Warm Inflation." *Physics of the Dark Universe* 27 (2020): 100432.

- [29] Yuennan, Jureeporn, and Phongpichit Channuie. "Further Refining Swampland Conjecture on Inflation in General Scalar-Tensor Theories of Gravity." *Fortschritte der Physik* 70.6 (2022): 2200024.
- [30] Bedroya, Alek, and Cumrun Vafa. "Trans-Planckian censorship and the swampland." *Journal of High Energy Physics* 2020.9 (2020): 1-34.
- [31] Sadeghi, Jafar, et al. "Can black holes cause cosmic expansion?." *arXiv preprint arXiv:2305.12545* (2023).
- [32] Mohammadi, Abolhassan, Tayeb Golanbari, and Jamil Enayati. "Brane inflation and Trans-Planckian censorship conjecture." *Physical Review D* 104.12 (2021): 123515.
- [33] Sadeghi, Jafar, Mohammad Reza Alipour, and Saeed Noori Gashti. "Scalar Weak Gravity Conjecture in Super Yang-Mills Inflationary Model." *Universe* 8.12 (2022): 621.
- [34] Kallosh, Renata, et al. "dS Vacua and the Swampland." *Journal of High Energy Physics* 2019.3 (2019): 1-18.
- [35] Guleriuz, Omer. "On the Trans-Planckian Censorship Conjecture and the generalized non-minimal coupling." *Journal of Cosmology and Astroparticle Physics* 2021.11 (2021): 043.
- [36] Osses, Constanza, Nelson Videla, and Grigoris Panotopoulos. "Reheating in small-field inflation on the brane: the swampland criteria and observational constraints in light of the PLANCK 2018 results." *The European Physical Journal C* 81 (2021): 1-29.
- [37] Sadeghi, J., S. Noori Gashti, and M. R. Alipour. "Notes on further refining de Sitter swampland conjecture with inflationary models." *Chinese Journal of Physics* 79 (2022): 490-502.
- [38] Brahma, Suddhasattwa. "Trans-Planckian censorship, inflation, and excited initial states for perturbations." *Physical Review D* 101.2 (2020): 023526.
- [39] Brandenberger, Robert. "Trans-Planckian censorship conjecture and early universe cosmology." *arXiv preprint arXiv:2102.09641* (2021).
- [40] Sadeghi, J., S. Noori Gashti, and F. Darabi. "Swampland conjectures in hybrid metric-Palatini gravity." *Physics of the Dark Universe* (2022): 101090.
- [41] Geng, Hao, Sebastian Grieninger, and Andreas Karch. "Entropy, entanglement and swampland bounds in DS/dS." *Journal of High Energy Physics* 2019.6 (2019): 1-16.
- [42] Gashti, S. Noori, J. Sadeghi, and B. Pourhassan. "Pleasant behavior of swampland conjectures in the face of specific inflationary models." *Astroparticle Physics* 139 (2022): 102703.
- [43] Sadeghi, J., E. Naghd Mezerji, and S. Noori Gashti. "Study of some cosmological parameters in logarithmic corrected $f(R)$ gravitational model with swampland conjectures." *Modern Physics Letters A* 36.05 (2021): 2150027.
- [44] Sadeghi, J., S. Noori Gashti, and E. Naghd Mezerji. "The investigation of universal relation between corrections to entropy and extremality bounds with verification WGC." *Physics of the Dark Universe* 30 (2020): 100626.
- [45] Agrawal, Prateek, et al. "On the cosmological implications of the string swampland." *Physics Letters B* 784 (2018): 271-276.
- [46] Odintsov, Sergei D., and Vasilis K. Oikonomou. "Swampland implications of GW170817-compatible Einstein-Gauss-Bonnet gravity." *Physics Letters B* 805 (2020): 135437.
- [47] Sadeghi, J., and S. Noori Gashti. "Investigating the logarithmic form of $f(R)$ gravity model from brane perspective and swampland criteria." *Pramana* 95 (2021): 1-8.
- [48] Sharma, Umesh Kumar. "Reconstruction of quintessence field for the THDE with swampland correspondence in $f(R, T)$ gravity." *International Journal of Geometric Methods in Modern Physics* 18.02 (2021): 2150031.
- [49] Sadeghi, Jafar, Mohammad Reza Alipour, and Saeed Noori Gashti. "Strong cosmic censorship in light of weak gravity conjecture for charged black holes." *Journal of High Energy Physics* 2023.2 (2023): 1-14.
- [50] Odintsov, S. D., V. K. Oikonomou, and L. Sebastiani. "Unification of constant-roll inflation and dark energy with logarithmic R^2 -corrected and exponential $F(R)$ gravity." *Nuclear Physics B* 923 (2017): 608-632.
- [51] Sadeghi, J., et al. "de Sitter Swampland Conjecture in String Field Inflation." *The European Physical Journal C* 83 (2023): (635).
- [52] Shokri, Mehdi, Jafar Sadeghi, and Saeed Noori Gashti. "Quintessential constant-roll inflation." *Physics of the Dark Universe* 35 (2022): 100923.
- [53] Sadeghi, J., et al. "Swampland conjecture and inflation model from brane perspective." *Physica Scripta* 96.12 (2021): 125317.
- [54] Noori Gashti, Saeed, Mohammad Reza Alipour, and Mohammad Ali S. Afshar. "Exploring the Parameter Space of Inflation Model on the Brane and its Compatibility with the Swampland Conjectures." *arXiv e-prints* (2024): arXiv:2409.
- [55] Sadeghi, J., et al. "The emergence of universal relations in the AdS black holes thermodynamics." *Physica Scripta* 98.2 (2023): 025305.
- [56] Sadeghi, Jafar, and Saeed Noori Gashti. "Influences of perfect fluid dark matter on coinciding validity of the weak gravity and weak cosmic censorship conjectures for Kerr-Newman black hole." *Nuclear Physics B* 1006 (2024): 116657.
- [57] Gashti, S. Noori, and J. Sadeghi. "Refined swampland conjecture in warm vector hybrid inflationary scenario." *The European Physical Journal Plus* 137.6 (2022): 1-13.
- [58] Kinney, William H. "Eternal inflation and the refined swampland conjecture." *Physical review letters* 122.8 (2019): 081302.
- [59] Sadeghi, Jafar, and Saeed Noori Gashti. "Reissner-Nordström black holes surrounded by perfect fluid dark matter: Testing the viability of weak gravity conjecture and weak cosmic censorship conjecture simultaneously." *Physics Letters B* 853 (2024): 138651.
- [60] Yu, Ten-Yeh, and Wen-Yu Wen. "Cosmic censorship and weak gravity conjecture in the Einstein-Maxwell-dilaton theory." *Physics Letters B* 781 (2018): 713-718.
- [61] Gashti, S. Noori. "Two-field inflationary model and swampland de Sitter conjecture." *Journal of Holography Applications in Physics* 2 (1) (2022): 13-24.
- [62] Vafa, Cumrun. "The String landscape and the swampland." *arXiv preprint hep-th/0509212* (2005).

- [63] Sadeghi, Jafar, et al. "Weak gravity conjecture from conformal field theory: a challenge from hyperscaling violating and Kerr-Newman-AdS black holes." *Chinese Physics C* 47.1 (2023): 015103.
- [64] van Beest, Marieke, et al. "Lectures on the swampland program in string compactifications." *Physics Reports* 989 (2022): 1-50.
- [65] Sadeghi, J., et al. "Weak gravity conjecture, black branes and violations of universal thermodynamics relation." *Annals of Physics* 447 (2022): 169168.
- [66] Kolb, Edward W., Andrew J. Long, and Evan McDonough. "Gravitino swampland conjecture." *Physical Review Letters* 127.13 (2021): 131603.
- [67] Yuennan, Jureeporn, and Phongpichit Channuie. "Further Refining Swampland Conjecture on Inflation in General Scalar-Tensor Theories of Gravity." *Fortschritte der Physik* 70.6 (2022): 2200024.
- [68] Palti, Eran. "The swampland: introduction and review." *Fortschritte der Physik* 67.6 (2019): 1900037.
- [69] Noori Gashti, S., J. Sadeghi, and M. R. Alipour. "Further refining swampland dS conjecture in mimetic $f(R)$ gravity." *International Journal of Modern Physics D* 32.03 (2023): 2350011.
- [70] Sadeghi, Jafar, et al. "Weak gravity conjecture from conformal field theory: a challenge from hyperscaling violating and Kerr-Newman-AdS black holes." *Chinese Physics C* 47.1 (2023): 015103.
- [71] Sadeghi, Jafar, et al. "Cosmic evolution of the logarithmic $f(R)$ model and the dS swampland conjecture." *Universe* 8.12 (2022): 623.
- [72] Sadeghi, Jafar, et al. "Weak cosmic censorship and weak gravity conjectures in CFT thermodynamics." *Journal of High Energy Astrophysics* 44 (2024): 482-493.
- [73] Alipour, Mohammad Reza, et al. "The interplay of WGC and WCCC via charged scalar field fluxes in the RPST framework." *Journal of High Energy Astrophysics* 45 (2025): 160-167.
- [74] Anand, Ankit. "Thermodynamic Extremality in Power-law AdS Black Holes A Universal Perspective." *arXiv preprint arXiv:2409.07079* (2024).
- [75] Gashti, Saeed Noori, Izzet Sakalli, and Behnam Pourhassan. "Thermodynamic topology, photon spheres, and evidence for weak gravity conjecture in charged black holes with perfect fluid within Rastall theory." *Physics Letters B* 869 (2025): 139862.
- [76] Anand, Ankit, et al. "Analyzing WGC and WCCC through charged scalar fields fluxes with charged AdS black holes surrounded by perfect fluid dark matter in the CFT thermodynamics." *Nuclear Physics B* 1013 (2025): 116857.
- [77] Alipour, Mohammad Reza, et al. "The interplay of WGC and WCCC via charged scalar field fluxes in the RPST framework." *Journal of High Energy Astrophysics* 45 (2025): 160-167.
- [78] Gashti, Saeed Noori, et al. "Noncommutativity and its role in constant-roll inflation models with non-minimal coupling constrained by swampland conjectures." *Chinese Physics C* 49.2 (2025): 025108-025108.
- [79] Sadeghi, Jafar, et al. "Weak cosmic censorship and weak gravity conjectures in CFT thermodynamics." *Journal of High Energy Astrophysics* 44 (2024): 482-493.
- [80] Alipour, Mohammad Reza, et al. "Weak Gravity Conjecture Validation with Photon Spheres of Quantum Corrected AdS-Reissner-Nordstrom Black Holes in Kiselev Spacetime." *arXiv preprint arXiv:2410.14352* (2024).
- [81] Sadeghi, Jafar, et al. "Swampland Conjectures and Noncommutative Phase Space in the Constant-roll Inflation with Brans-Dicke Cosmology." *International Journal of Theoretical Physics* 63.12 (2024): 1-20.
- [82] Afshar, Mohammad Ali S., and Jafar Sadeghi. "Black Hole Orbit Classification: The Synergistic Effects of Cloud Strings, Gauss-Bonnet Terms, and Non-Commutative Parameters in Identifying WGC candidate Models: WGC as WCCC protector." *arXiv preprint arXiv:2412.00079* (2024).
- [83] Gashti, Saeed Noori, and Behnam Pourhassan. "Cosmic-quantum connections: Assessing the viability of weak gravity and weak cosmic censorship conjectures in Kerr-Newman-Kiselev-Letelier black hole." *Physics Letters B* (2025): 139730.
- [84] Penrose, Roger. "Gravitational collapse and space-time singularities." *Physical Review Letters* 14.3 (1965): 57.
- [85] Harlow, Daniel, et al. "The weak gravity conjecture: a review." *arXiv preprint arXiv:2201.08380* (2022).
- [86] Shaymatov, Sanjar, Bobomurat Ahmedov, and Mubasher Jamil. "Testing the weak cosmic censorship conjecture for a Reissner-Nordström-de Sitter black hole surrounded by perfect fluid dark matter." *The European Physical Journal C* 81 (2021): 1-11.
- [87] Riess, Adam G., et al. "Observational evidence from supernovae for an accelerating universe and a cosmological constant." *The astronomical journal* 116.3 (1998): 1009.
- [88] Farrah, Duncan, et al. "Observational evidence for cosmological coupling of black holes and its implications for an astrophysical source of dark energy." *The Astrophysical Journal Letters* 944.2 (2023): L31.
- [89] Wei, Shao-Wen. "Topological charge and black hole photon spheres." *Physical Review D* 102.6 (2020): 064039.
- [90] Cunha, Pedro VP, Emanuele Berti, and Carlos AR Herdeiro. "Light-ring stability for ultracompact objects." *Physical review letters* 119.25 (2017): 251102.
- [91] Noori Gashti, Saeed, et al. "Assessing WGC Compatibility in ModMax Black Holes via Photon Spheres Analysis and WCCC Validation." *arXiv e-prints* (2025): arXiv-2504.
- [92] Sekhmani, Yassine, et al. "Thermodynamic topology of Black Holes in $F(R)$ -Euler-Heisenberg gravity's Rainbow." *arXiv preprint arXiv:2409.04997* (2024).
- [93] Panah, B. Eslam, S. Zare, and H. Hassanabadi. "Accelerating AdS black holes in gravity's rainbow." *The European Physical Journal C* 84.3 (2024): 259.
- [94] Eslam Panah, B., B. Hazarika, and P. Phukon. "Thermodynamic topology of topological black hole in $F(R)$ -ModMax gravity's rainbow." *Progress of Theoretical and Experimental Physics* 2024.8 (2024): 083E02.
- [95] Panah, Behzad Eslam, et al. "Super-entropic black holes in gravity's rainbow and determining constraints on rainbow functions." *The European Physical Journal C* 85.6 (2025): 650.

- [96] Lin-fang, Deng, Zhang He-Yao, and Long Chao-Yun. "Particle collisions around static spherically symmetric black hole and rotating black hole in gravity's rainbow." arXiv preprint arXiv:2505.23874 (2025).
- [97] Naskar, Sayan, Niyaz Uddin Molla, and Ujjal Debnath. "Strong gravitational lensing by black hole in F (R)-Euler–Heisenberg Gravity's Rainbow." *Physics of the Dark Universe* (2025): 102009.
- [98] Araújo Filho, A. A., et al. "Gravitational lensing by a lorentz-violating black hole." *The European Physical Journal Plus* 140.11 (2025): 1117.
- [99] Wang, Yiyang, et al. "Strong gravitational lensing by static black holes in effective quantum gravity." *The European Physical Journal C* 85.3 (2025): 1-18.
- [100] Liu, Hao, et al. "Gravitational lensing effect of black holes in effective quantum gravity." *Physical Review D* 110.10 (2024): 104039.
- [101] Vachher, Amnish, Arun Kumar, and Sushant G. Ghosh. "The influence of uniform magnetic fields on strong field gravitational lensing by Kerr black holes." *Journal of Cosmology and Astroparticle Physics* 2025.11 (2025): 021.
- [102] Lan, Yi-Ling, et al. "Gravitational lensing by a charged black hole with a global monopole in the strong field limit." *Physical Review D* 111.8 (2025): 084079.
- [103] Heidari, Narges, and Jarley P. Lobo. "Black Hole Gravitational Phenomena in Higher-Order Curvature-Scalar Gravity." arXiv preprint arXiv:2509.11985 (2025).
- [104] Mushtaq, Farzan, et al. "Imprints of magnetic charge on the particle orbits, weak gravitational lensing and black hole shadows." *Physics of the Dark Universe* (2025): 102109.
- [105] Afshar, Mohammad Ali S., and Jafar Sadeghi. "Mechanisms behind the Aschenbach effect in non-rotating black hole spacetime." *Annals of Physics* (2025): 169953.
- [106] Afshar, Mohammad Ali S., and Jafar Sadeghi. "Mutual influence of photon sphere and non-commutative parameter in various non-commutative black holes: Towards evidence for WGC." *Physics of the Dark Universe* 47 (2025): 101814.
- [107] Alipour, Mohammad Reza, et al. "Weak gravity conjecture validation with photon spheres of quantum corrected Reissner–Nordstrom–AdS black holes in Kiselev spacetime." *The European Physical Journal C* 85.2 (2025): 138.
- [108] Sadeghi, Jafar, and Mohammad Ali S. Afshar. "The role of topological photon spheres in constraining the parameters of black holes." *Astroparticle Physics* 162 (2024): 102994.
- [109] Alipour, Mohammad Reza, et al. "Reconciling the Weak Gravity and Weak Cosmic Censorship Conjectures in Einstein–Euler–Heisenberg–AdS Black Holes." arXiv preprint arXiv:2504.03453 (2025).
- [110] Dehghani, M. "AdS4 black holes with nonlinear source in rainbow gravity." *Physics Letters B* 801 (2020): 135191.
- [111] Dehghani, M. "Thermodynamics of $(2+1)$ -dimensional charged black holes with power-law Maxwell field." *Physical Review D* 94.10 (2016): 104071.
- [112] Zangeneh, M. Kord, M. H. Dehghani, and A. Sheykhi. "Thermodynamics of topological black holes in Brans–Dicke gravity with a power-law Maxwell field." *Physical Review D* 92.10 (2015): 104035.
- [113] Dehghani, M. "Thermal fluctuations of dilaton black holes in gravity's rainbow." *Physics Letters B* 781 (2018): 553-560.
- [114] Jacob, Uri, et al. "Modifications to Lorentz invariant dispersion in relatively boosted frames." *Physical Review D—Particles, Fields, Gravitation, and Cosmology* 82.8 (2010): 084021.
- [115] Amelino-Camelia, Giovanni. "Quantum-spacetime phenomenology." *Living Reviews in Relativity* 16.1 (2013): 5.
- [116] Dehghani, M. "Thermodynamics of novel charged dilaton black holes in gravity's rainbow." *Physics Letters B* 785 (2018): 274-283.
- [117] Jusufi, K., Sakalli, İ., and Övgün, A. "Effect of Lorentz symmetry breaking on the deflection of light in a cosmic string spacetime." *Physical Review D* 96.2 (2017): 024040.
- [118] Sucu, E. and Sakalli, İ. "Charged regular black holes in quantum gravity: from thermodynamic stability to observational phenomena." *European Physical Journal C* 85.9 (2025): 989.
- [119] Sucu, E. and Sakalli, İ. "Quantum-corrected thermodynamics and plasma lensing of MOG black holes." *Proceedings of the Royal Society A* 481.2320 (2025): 20250251.
- [120] Ahmed, F., Al-Badawi, A., and Sakalli, İ. "Photon spheres, gravitational lensing/mirroring, and greybody radiation in deformed AdS–Schwarzschild black holes with phantom global monopole." *Physics of the Dark Universe* 49 (2025): 101988.
- [121] Ahmed, F., Sakalli, İ., and Al-Badawi, A. "Gravitational lensing phenomena of Ellis–Bronnikov–Morris–Thorne wormhole with global monopole and cosmic string." *Physics Letters B* 864 (2025): 139448.
- [122] Sucu, E. and Sakalli, İ. "Astrophysical reality of black hole thermodynamics and dynamics: Transformative influence of Hernquist dark matter distributions." *Physics of the Dark Universe* 49 (2025): 102051.
- [123] Sucu, E. and Sakalli, İ. "Exploring Lorentz-violating effects of Kalb–Ramond field on charged black hole thermodynamics and photon dynamics." *Physical Review D* 111.6 (2025): 064049.